Hydrostatic Pressures Developed by Osmotically Swelling Vesicles Bound to Planar Membranes

WALTER D. NILES, FREDRIC S. COHEN, and ALAN FINKELSTEIN

From the Rush Medical College, Department of Physiology, Chicago, Illinois 60612; and the Albert Einstein College of Medicine, Departments of Physiology and Biophysics, and Neuroscience, Bronx, New York 10461

ABSTRACT When phospholipid vesicles bound to a planar membrane are osmotically swollen, they develop a hydrostatic pressure (ΔP) and fuse with the membrane. We have calculated the steady-state ΔP, from the equations of irreversible thermodynamics governing water and solute flows, for two general methods of osmotic swelling. In the first method, vesicles are swollen by adding a solute to the vesicle-containing compartment to make it hyperosmotic. ΔP is determined by the vesicle membrane's permeabilities to solute and water. If the vesicle membrane is devoid of open channels, then ΔP is zero. When the vesicle membrane contains open channels, then ΔP peaks at a channel density unique to the solute permeability properties of both the channel and the membrane. The solute enters the vesicle through the channels but leaks out through the region of vesicle-planar membrane contact. ΔP is largest for channels having high permeabilities to the solute and for solutes with low membrane permeabilities in the contact region. The model predicts the following order of solutes producing pressures of decreasing magnitude: KCl > urea > formamide ≥ ethylene glycol. Differences between osmoticants quantitatively depend on the solute permeability of the channel and the density of channels in the vesicle membrane. The order of effectiveness is the same as that experimentally observed for solutes promoting fusion. Therefore, ΔP drives fusion. When channels with small permeabilities are used, coupling between solute and water flows within the channel has a significant effect on ΔP. In the second method, an impermeant solute bathing the vesicles is isosmotically replaced by a solute which permeates the channels in the vesicle membrane. ΔP resulting from this method is much less sensitive to the permeabilities of the channel and membrane to the solute. ΔP approaches the theoretical limit set by the concentration of the impermeant solute.

INTRODUCTION

Swelling of phospholipid vesicles bound to a planar membrane leads to fusion (Cohen et al., 1980; Zimmerberg et al., 1980; Cohen et al., 1982; Akabas et al.,

Address reprint requests to Dr. Fredric S. Cohen, Department of Physiology, Rush Medical College, 1753 West Congress Parkway, Chicago, IL 60612-3864.

J. GEN. PHYSIOL. © The Rockefeller University Press · 0022-1295/89/02/0211/34 $2.00
Volume 93 February 1989 211–244

1984). When swelling is induced by establishing an osmotic gradient across the planar membrane, with the vesicle-containing (*cis*) compartment hyperosmotic with respect to the other (*trans*) compartment, channels are required in the vesicular membrane for fusion to occur (Woodbury, 1986; Niles and Cohen, 1987). The ability of the osmoticant (the solute used to establish the osmotic gradient) to promote fusion depends on its permeability through the bare bilayer and the channel (Cohen et al., 1989). However, when bound vesicles are swollen by replacing their *cis* compartment medium of a channel-impermeant solute with a channel-permeant solute, the extent of fusion is relatively independent of the permeability of the solute through bare bilayer (Cohen et al., 1989).

In this paper we use the formalism of irreversible thermodynamics to write expressions for the flows of water and solutes across the vesicular and planar membranes, for all experimentally realized configurations. We calculate the steady-state intravesicular pressure, ΔP, generated in each configuration. In the absence of channels, pressures do not develop. In the presence of channels, these calculated pressures correctly predict the potencies of solutes in promoting fusion. We therefore conclude that the intravesicular pressures drive fusion. Ion channels are routinely reconstituted into planar membranes by fusion methods. Commonly, swelling and fusion are induced with an osmotic gradient across the planar membrane (cf. Moczydlowski and Latorre, 1983; Cohen, 1986). The model presented allows optimal reconstitution conditions to be calculated.

THEORY

Definitions

The planar membrane separates two compartments containing initially identical solutions. The side to which the vesicles are added (the *cis* compartment) is termed compartment 2, while the *trans*-side of the planar membrane is compartment 1 (see Fig. 1). The initial solute, present in both compartments and inside the vesicle, is typically, but not always, a bilayer-impermeant electrolyte, such as KCl. Osmoticants added to compartment 2 (making it hyperosmotic) include salts and nonelectrolytes.

The vesicle is modeled as being fully swollen and directly abutted against the planar membrane. The vesicle's surface is thus divided into two distinct regions (Fig. 1). The contact region has area A_1, which is a constant fraction, f, of the vesicle membrane's total surface area A. The noncontact region (bathed by the buffer of compartment 2) has surface area A_2. In all cases, channels embedded in the vesicle membrane are confined to the noncontact region. The fully swollen vesicle initially has neither any tension on its membrane nor an intravesicular hydrostatic pressure.

Water and Solute Fluxes across a Membrane

We assume that across any region of vesicle membrane, water and solute flows are governed by driving forces as described by the equations of irreversible thermodynamics (Kedem and Katchalsky, 1958). For volume (water) flow, J_v, the driving forces are the differences in osmotic and hydrostatic pressures across the mem-

brane,

$$J_v = L(RT\sigma\lambda\Delta c - \Delta P), \tag{1}$$

where Δc is the concentration difference between the inside of the vesicle and another compartment of all osmotically active solutes, ΔP is the hydrostatic pressure difference between the inside of the vesicle and the outside solutions, and L is the hydraulic permeability coefficient of the membrane region. σ is the reflection coefficient, which indicates the extent of coupling between the flows of water and solute, such that maximum interaction occurs for $\sigma = 0$. The molecularity λ relates the molality of a solute to its osmolality ($\lambda = 2$ if one mole of a binary solute dissociates into two osmoles of osmotically active particles, e.g., KCl). The flow of solute, J_n, is driven by the solute concentration difference across the membrane and by any convective flow of water to which the solute is coupled. Thus,

$$J_n = -\omega RT\Delta c + (1 - \sigma)\bar{c}J_v, \tag{2}$$

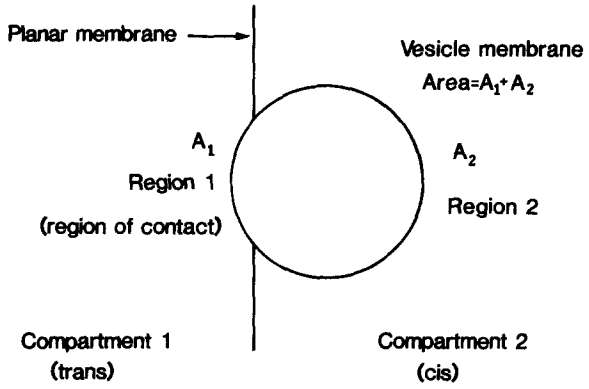

FIGURE 1. Membrane regions and bathing compartments defined for a vesicle bound to a planar membrane. The two compartments bathe opposite sides of the planar membrane. Compartment 2 is the *cis* compartment to which vesicles are added, while the opposite side of the planar membrane (*trans*) is compartment 1. A constant fraction (f) of the vesicle's total surface area (A) is actually bound to the planar membrane, facing compartment 1 and forming the region of contact with area A_1. The remainder of the vesicle's membrane, facing compartment 2, is the noncontact region; its area is A_2. For the purposes of simulating permeability properties, the contact region is modeled as being comprised of a single lipid bilayer.

where ω is the solute permeability coefficient for the membrane region, and $\bar{c}$ is the average solute concentration of the two compartments separated by the membrane region. By these definitions, a flow into the vesicle has a positive sign.

The permeability coefficients L and ω for bare lipid bilayer are obtained from intrinsic permeability coefficients. For the i-th membrane region with area A_i, $L_i = P_f A_i \bar{V}_w/RT$, where P_f is the permeability coefficient of lipid bilayer membrane to water flow, $\bar{V}_w$ is the partial molar volume of water, and R and T have their usual meanings. For the flow of a solute across the same region, $\omega_i = P_d A_i/RT$, where P_d is the permeability coefficient of the region to the solute. In our model, L_1 and ω_1 are the permeability coefficients of the region of contact, which faces compartment 1, while L_2 and ω_2 are the permeability coefficients of the noncontact region (facing

compartment 2).[1] It is experimentally known that ω/L is, to first order, independent of lipid composition, as expected from Overton's rule, as both water and solute cross bilayers by a solubility-diffusion mechanism (Finkelstein, 1976). All values of P_d and P_f that we use are listed in Finkelstein (1987).

When transmembrane channels span the noncontact region, the permeability coefficients (L and ω) are the sums of the coefficients for the unmodified lipid bilayer part of the region and for the channels embedded in it. In our model, we use porin and double-sided nystatin for channels, because these have been used in our experiments (Cohen et al., 1984; Niles and Cohen, 1987). The permeability coefficients for water and a number of nonelectrolytes have been measured for bare lipid bilayers (Finkelstein, 1976; Fettiplace and Haydon, 1980; Orbach and Finkelstein, 1980; Walter and Gutknecht, 1986; Finkelstein, 1987) as well as for double-sided nystatin channels (Cass and Finkelstein, 1967; Holz and Finkelstein, 1970). The sieving radius has been measured for porin (Nikaido and Rosenberg, 1981). We estimate porin's permeabilities to nonelectrolytes from this radius, and its permeability to electrolytes from the ionic conductance and selectivity as elaborated in the Appendix. We examine four specific cases for inducing osmotic swelling, which correspond to actual experimental configurations. In each case, we calculate the intravesicular pressure ΔP, which drives fusion.

Case I: No Channels

Consider a vesicle, with no channels in its membrane, bound to the planar membrane. A single bilayer-permeant solute is present in compartments 1 and 2 and inside the vesicle at identical concentrations. For simplicity, the solute is a simple nonelectrolyte, so that $\lambda = 1$. Thus, $c_2 = c_v = c_1$, initially, where c_v is the concentration of the solute inside the vesicle. The *cis* compartment is made hyperosmotic ($c_2 > c_1$) by adding more of the same solute (see Fig. 2). The flow of water is described by

$$J_v = L_2[RT(c_v - c_2) - \Delta P] + L_1[RT(c_v - c_1) - \Delta P] \tag{3}$$

and the flow of the solute is given by

$$J_n = \omega_2 RT(c_2 - c_v) + \omega_1 RT(c_1 - c_v). \tag{4}$$

Solute and water flux coupling is neglected because the reflection coefficients of typical nonelectrolytes measured in pure lipid bilayers equal 1 (cf. Finkelstein, 1987).

The flux equations are solved for the hydrostatic pressure and c_v at steady state, when $J_v = J_n = 0$. It is found that $c_v = (\omega_2 c_2 + \omega_1 c_1)/(\omega_2 + \omega_1)$ and $\Delta P = RT[c_v - (L_2 c_2 + L_1 c_1)/(L_2 + L_1)]$. Substitution for c_v in the latter expression yields

$$\Delta P = RT\left[\frac{\omega_1 L_2 - \omega_2 L_1}{(\omega_1 + \omega_2)(L_1 + L_2)}\right](c_1 - c_2). \tag{5}$$

[1] We treat the region of contact as having the permeability properties of a single bare lipid bilayer. Channels do not span the membrane in the region of contact experimentally (Niles and Cohen, 1987).

But $\omega_1 L_2 - \omega_2 L_1 = 0$, because $\omega_1/L_1 = \omega_2/L_2$, and, hence, $\Delta P = 0$.[2] Qualitatively, when the medium surrounding a vesicle without channels is made hyperosmotic, solute and water flow into and out of the vesicle until a value of c_v is reached, intermediate between c_2 and c_1. At this concentration the rate of solute influx into the vesicle from compartment 2 equals the rate of solute efflux out of the vesicle across the contact region into compartment 1, and similarly the osmotic influx of water from compartment 1 equals the osmotic efflux of water from the vesicle into compartment 2. This steady-state condition is achieved with an intravesicular ΔP of zero, and the vesicle is shrunken from its originally fully swollen state.

Channels in the Noncontact Region

It is evident from Eq. 5 that nonzero pressures will develop in the vesicle when $\omega_1/L_1 \neq \omega_2/L_2$. The condition $\omega_2/L_2 > \omega_1/L_1$ occurs when channels exist in the

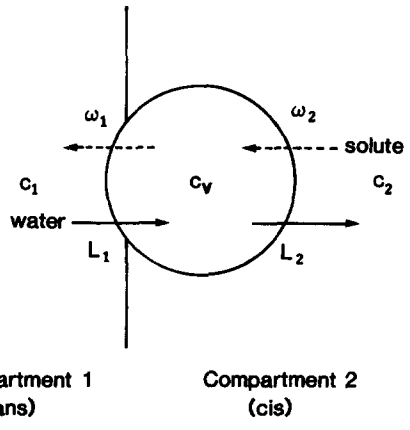

FIGURE 2. Case I. Attempted hyperosmotic swelling of a vesicle without channels. Both compartments and the vesicle contain the same solute, which is initially at the same concentration everywhere. c_2 is the solute concentration in compartment 2, c_v is that inside the vesicle, and c_1 is that in compartment 1. Swelling is attempted by making $c_2 > c_1$ with the addition of solute to compartment 2. Each subscript on the solute (ω) and hydraulic (L) permeability coefficients refers to the compartment faced by the indicated region of vesicle membrane. The solid and broken arrows denote the directions of the flows of water and solute, respectively, at steady state. The flow of water is determined entirely by the osmotic gradients between the inside of the vesicle and compartments 1 and 2; the net intravesicular pressure is zero.

noncontact region of the vesicle membrane. Channels increase ω_2 with a minimal increase in L_2. This results because water, in contrast to the nonelectrolytic solutes, is fairly permeant through phospholipid bilayers. P_f is $\sim 10^{-3}$ cm/s for phosphatidylcholine (PC) bilayers painted from decane ($\sim 10^{-4}$ cm/s for PC/sterol:1/1 by mole fraction; Finkelstein, 1976) as compared with nonelectrolytes, such as urea, glycerol, and formamide with P_d's of 4×10^{-6}, 5.4×10^{-6}, and 1.03×10^{-4} cm/s, respec-

[2] That the hydrostatic pressure is zero in this simple model can also be shown from the definitions of L and ω in terms of the fraction of the vesicle surface area comprising the contact area. Since $f = A_1/(A_1 + A_2) = \omega_1/(\omega_1 + \omega_2) = L_1/(L_1 + L_2)$ and $1 - f = A_2/(A_1 + A_2) = \omega_2/(\omega_1 + \omega_2) = L_2/(L_1 + L_2)$, $c_v = fc_1 + (1 - f)c_2$ and $\Delta P = RT[c_v - fc_1 - (1 - f)c_2] = 0$. Although this method uses implicitly the invariance of the permeability ratio ω/L from region to region of the vesicle membrane, the treatment given in the text emphasizes that the condition $\Delta P = 0$ is dependent on the assumption that $\omega_1/L_1 = \omega_2/L_2$; that is, the relative permeability of the contact region to solute and water is the same as that in the noncontact region.

tively. Adding a few channels to the membrane does not increase L to any great extent but will significantly increase ω. The presence of channels increases the rate at which solute enters the vesicle from compartment 2 and leads to a higher steady-state c_v. This leads to an increased osmotic flux of water into the vesicle (from compartment 1) and to a decreased osmotic efflux into compartment 2, as is depicted in Fig. 3. The only way for a vesicle with channels to attain a steady-state volume flux is to develop a ΔP; water entering the vesicle from compartment 1 is forced out of the vesicle into compartment 2 by this ΔP (Fig. 3). Adding too many channels leads to a decrease in ΔP. The hydraulic permeability increases to such an extent that the development of even a small ΔP results in a significant pressure-driven efflux of solute and water from the vesicle. There is thus a channel density that leads to maximum pressures.

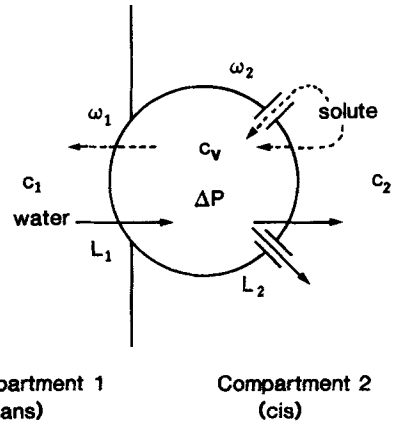

FIGURE 3. Hyperosmotic swelling of a vesicle with channels embedded in the noncontact region. The concentrations and bilayer permeability coefficients (ω's and L's) have the same meaning as in Fig. 2. The only difference between this situation and that depicted in Fig. 2 is the presence of two channels in the noncontact region of the vesicle membrane. Before the start of the experiment, $c_1 = c_v = c_2$. The experiment is started by making $c_2 > c_1$. The solid and broken arrow denote the directions of water and solute flows, respectively, at steady state. At steady state, solute diffuses into the vesicle from compartment 2 through the channels and the bilayer of the noncontact region. The steady-state water influx into the vesicle results from the osmotic gradient between the vesicle and compartment 1 ($c_v \gg c_1$). Because the channels allow for a larger solute influx, $c_v \cong c_2$, the osmotic gradient between the vesicle and compartment 2 is too small to set up a steady-state water efflux from the vesicle. Instead, this efflux of water arises from an intravesicular hydrostatic pressure (ΔP) which builds up to force water out of the vesicle into compartment 2.

When channels are present, we adopt a double-subscripted notation for concentrations (see Fig. 4). Initially, both compartments and the vesicle are filled with the initial solute (subscript s), which is bilayer impermeant. The experiment is started by adding a permeant osmoticant (subscript p) to compartment 2, making it hyperosmotic. The concentration of the i-th solute in the j-th compartment is denoted by $c_{i,j}$. Thus $c_{p,v}$ and $c_{p,2}$ are the concentrations of the osmoticant in the vesicle and compartment 2, respectively, while $c_{s,v}$ and $c_{s,2}$ are those of the initial solute. Osmoticant is added only to compartment 2, and its concentration in compartment 1 ($c_{p,1}$) remains negligible despite leakage from the vesicle. We let $c_{p,1} = 0$, and the concentration of the initial solute in compartment 1 is denoted by $c_{s,1}$. The molecularity of the initial solute is denoted by λ_s and that of the osmoticant by λ_p. The permeabilities of the channels to the initial solute and the osmoticant are ω_s and ω_p, and the

reflection coefficients are σ_s and σ_p, respectively. The hydraulic permeability for all the channels in the noncontact region of the vesicle is denoted by L_p.[3] L_1, L_2, ω_1, and ω_2 retain their meanings from the previous section; that is, they are the hydraulic and osmoticant (p) permeability coefficients through the vesicle bilayer in the region of contact (subscript 1) and the noncontact region (subscript 2).

Case II: Channels and a Permeant Initial Solute

We let the initial solute and the added osmoticant be permeants of the channels that span the vesicular membrane. We assume the initial solute is bilayer impermeant. This models experiments in which porin is incorporated into the vesicle membrane (Akabas et al., 1984; cf. Cohen et al., 1980) and many reconstitution experiments (cf. Moczydlowski and Latorre, 1983). As in all of the cases considered, the channels

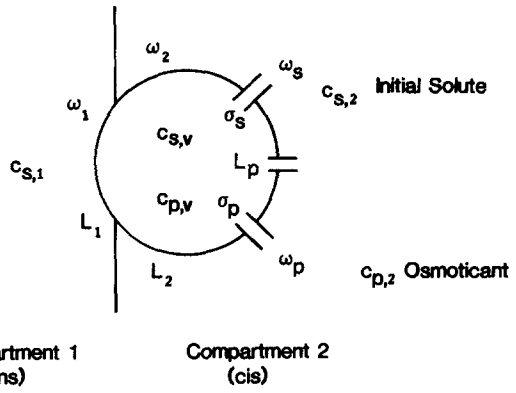

FIGURE 4. Case II. Hyperosmotic swelling of a vesicle with large channels in its membrane bathed in a channel-permeating solute. The channel-permeant but lipid bilayer-impermeant initial solute is present at concentrations $c_{s,1}$ in compartment 1, $c_{s,v}$ inside the vesicle, and $c_{s,2}$ in compartment 2. Its solute permeability coefficient through all of the channels is ω_s with reflection coefficient σ_s. The experiment is started by adding a channel-permeating (channel permeability coefficient ω_p) and possibly lipid bilayer-permeating osmoticant to compartment 2. The osmoticant concentration in compartment 2 is $c_{p,2}$ and inside the vesicle it is $c_{p,v}$. The reflection coefficient of the osmoticant in the channel is σ_p. The hydraulic permeability coefficient of the channels is L_p. In the steady state, the osmoticant enters the vesicle through the channels and the vesicle bilayer in the noncontact region and water enters the vesicle from compartment 1 ($c_{p,v} + c_{s,v} > c_{s,1}$). To achieve a steady-state efflux of water, a ΔP develops to force the water from the vesicle into compartment 2.

are confined to the noncontact region of the vesicle (see Fig. 4), and the vesicle is initially at full volume. The initial solute is at the same concentrations in all compartments ($c_{s,1} = c_{s,v} = c_{s,2}$), and, at time $t = 0$, osmoticant is added to compartment 2. The equation for volume flow is

$$J_v = L_1\{RT[\lambda_s(c_{s,v} - c_{s,1}) + \lambda_p c_{p,v}] - \Delta P\} + L_2\{RT[\lambda_s(c_{s,v} - c_{s,2}) + \lambda_p(c_{p,v} - c_{p,2})] - \Delta P\} + L_p\{RT[\sigma_s\lambda_s(c_{s,v} - c_{s,2}) + \sigma_p\lambda_p(c_{p,v} - c_{p,2})] - \Delta P\}.^4 \quad (6)$$

[3] The subscript "p" in L_p denotes "pressure," not "permeant"; we hope this causes no confusion.

[4] We neglect any contributions of electro-osmosis and streaming potentials to volume and salt fluxes through the channels.

The flux of the initial solute is

$$J_s = \omega_s RT(c_{s,2} - c_{s,v}) + (1/2)\,(1 - \sigma_s)(c_{s,2} + c_{s,v})L_p \cdot \{RT[\sigma_s\lambda_s(c_{s,v} - c_{s,2}) + \sigma_p\lambda_p(c_{p,v} - c_{p,2})] - \Delta P\} \quad (7)$$

and the flux of the osmoticant is given by

$$J_p = -\omega_1 RTc_{p,v} + \omega_2 RT(c_{p,2} - c_{p,v}) + \omega_p RT(c_{p,2} - c_{p,v}) + (1/2)(1 - \sigma_p) \cdot (c_{p,v} + c_{p,2})L_p\{RT[\sigma_s\lambda_s(c_{s,v} - c_{s,2}) + \sigma_p\lambda_p(c_{p,v} - c_{p,2})] - \Delta P\}. \quad (8)$$

The convective flux term in each equation is confined to the channels. This system of coupled equations is tractable analytically when the osmoticant is the same species as the initial solute, in which case the three equations reduce to two, and they can be solved for the steady-state pressure. For the general case, numerical integration is more convenient than solving the resulting quartic equation for the steady-state ΔP and allows the time course for shrinking and swelling to be followed.

The number of solute particles initially inside the vesicle is $n_0 = c_{s,v}V_0$, where V_0 is the initial volume, and the number of osmoticant particles is zero. We increment time by steps of Δt, evaluate Eqs. 6–8 using the values of $c_{s,v}$ and $c_{p,v}$ obtained from the prior step, and increment V and the number of solute and osmoticant particles according to Eq. 9. At time $t = n\Delta t$,

$$V(t) = V_0 + \sum_{i-1}^{n} J_v(i)\Delta t,\ c_{s,v}(t) = \frac{n_0 + \sum_{i-1}^{n} J_S(i)\Delta t}{V(t)},$$

and

$$c_{p,v}(t) = \frac{\sum_{i-1}^{n} J_p(i)\Delta t}{V(t)}, \quad (9)$$

where $J_v(i)$, $J_s(i)$, and $J_p(i)$ are the fluxes of volume, the initial solute, and the osmoticant (Eqs. 6–8) evaluated at the start of the i-th time interval. During the initial shrinking and subsequent swelling, $\Delta P = 0$. Once the vesicle has reswollen to V_0, we set $J_v = 0$ because phospholipid bilayer membranes are relatively indistensible (Evans and Skalak, 1983). Eq. 6 is then solved for the pressure corresponding to the current values of $c_{s,v}$ and $c_{p,v}$. This value of ΔP is in turn substituted into the solute flux equations (7 and 8) to obtain the values of $c_{s,v}$ and $c_{p,v}$ at the next time increment. This iteration is repeated until ΔP, $c_{s,v}$, and $c_{p,v}$ converge to their steady-state values, defined as when an iteration produces a change in value of less than one part in ten thousand.

Time courses of shrinking and swelling for two vesicles, one 50 nm and the other 1 μm in radius, under identical osmotic conditions are shown in Fig. 5, in which V, $\lambda_s c_{s,v}$, $\lambda_p c_{p,v}$, and ΔP are plotted against time. The conditions are 100 mM KCl as the initial solute and 200 mM urea as the osmoticant. Each vesicle has 20% of its total surface area in contact with the planar membrane; the noncontact region contains one porin channel, modeled as a pipe through which the solutes can freely diffuse (see Appendix). Although the osmolality is doubled by the addition of urea, the 50-

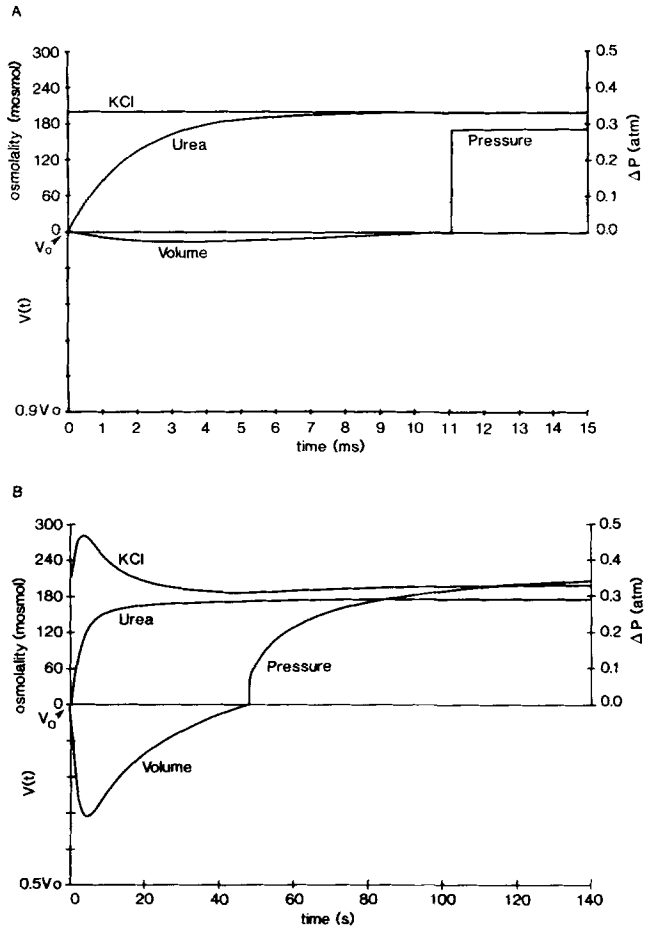

FIGURE 5. Time courses of shrinking and swelling for two vesicles of radius 50 nm (*A*) and 1 μm (*B*) for case II after compartment 2 is made 200 mosmol hyperosmotic with urea. In each panel, the volume of the vesicle (V), the osmolality of initial solute (KCl) inside the vesicle ($2c_{s,v}$, because $\lambda_s = 2$), the osmolality of osmoticant inside the vesicle ($c_{p,v}$), and the intravesicular pressure (ΔP) are plotted against time. Note the different time scales in *A* (milliseconds) and *B* (seconds). In both *A* and *B*, V is plotted along the ordinate at the lower left, $c_{s,v}$ and $c_{p,v}$ along the upper left ordinate, and ΔP along the right-hand ordinate. The vesicles initially contain 100 mM KCl, have 20% of their surface areas in contact with the planar membrane, and have one porin channel (modeled as a pipe) in the noncontact region (see Appendix). In *A*, $\omega_1 = 1.014 \times 10^{-26}$ mol·cm^3/erg·s, $\omega_2 = 4.055 \times 10^{-26}$, $L_1 = 1.004 \times 10^{-22}$ cm^6/erg·s, and $L_2 = 4.014 \times 10^{-22}$. In *B*, $\omega_1 = 4.055 \times 10^{-24}$, $\omega_2 = 1.622 \times 10^{-23}$, $L_1 = 4.014 \times 10^{-20}$, and $L_2 = 1.606 \times 10^{-19}$ (the membrane permeability coefficients for PC were obtained from Finkelstein, 1976), In both *A* and *B*, $\omega_p = 1.177 \times 10^{-23}$, $\omega_s = 5.516 \times 10^{-24}$, $L_p = 1.200 \times 10^{-21}$, and the reflection coefficients of both urea and KCl are 0.1. In both examples, as soon as the vesicle has reswollen to its initial volume (V_0), ΔP reaches significant values (>0.1 atm) very quickly.

nm radius vesicle (Fig. 5 *A*) shrinks by <1% to its minimum volume within 3 ms. Similarly, the concentration of KCl in the vesicle transiently increases by this percentage. The urea concentration inside the vesicle increases from 0 to 160 mM (at the minimum volume) during the shrinking epoch. Any shrinkage due to the osmotic gradient between the vesicle and compartment 2 and any influx of urea, increases the osmolality of the vesicle. This increases the osmotic influx of water through the contact region and keeps shrinkage to a minimum. The continued influx of urea and water reswells the vesicle to V_0 within 11 ms after the initial osmotic shock. At this point further entry of water and urea causes a rapid increase in ΔP (due to the indistensibility of the membrane), reaching to within 1% of its steady-state value of 0.28 atm within 0.1 μs. $c_{p,v}$ is ~199.5 mM at steady state. The step increase in ΔP when $V(t) = V_0$ is a consequence of the assumed inelasticity of the vesicle membrane; the finite dV/dt that exists when the vesicle reaches V_0 is brought to zero by this step in ΔP. Once the vesicle has reswollen to its initial volume, it can no longer expand; further entry of urea no longer causes the vesicle's volume to increase. Instead, the vesicle develops a ΔP that opposes any further volume increase due to the influx of water through the contact region and the water accompanying urea entry.

The time course of shrinking and swelling depends on the radius of the vesicle and the density of channels in the vesicle membrane. This is illustrated in Fig. 5 *B*, where the cycle is plotted for a 1-μm-radius vesicle under the same conditions as in Fig. 5 *A*. Shrinking, swelling, and pressure development are much slower (the cycle taking ~2 min), and the concentration changes in the vesicle are greater. During the first 4 s, the volume decreases by 32% and the KCl and urea concentrations in the vesicle rise to 130 and 132 mM, respectively. The vesicle takes ~45 s to reswell to V_0. Although the hydrostatic pressure instantaneously reaches 0.08 atm after V_0 is attained, it takes nearly 100 s to attain the steady-state value of 0.34 atm. Steady state is reached with a lower urea concentration in the vesicle (175 mM). All of these effects result from the reduced channel density, which slows the rate at which $c_{p,v}$ increases. A 1-μm-radius vesicle has 8,000 times the volume of the 50-nm vesicle, and accordingly the latter vesicle swells ~10,000 times faster than the former. The time course can be shortened by placing 8,000 channels in the large vesicle. In this case, swelling occurs with approximately the same time course as with the 50-nm vesicle.

The magnitude of the steady-state ΔP depends on the bilayer permeability of the osmoticant. This is shown in Table I, in which the ΔP resulting from a 200 mosmol/kg gradient of the indicated osmoticant is tabulated for vesicles 100-nm and 1-μm in radius (each vesicle contains one porin channel). The largest pressures are obtained with KCl, which is impermeant through the lipid bilayer. Urea is the next most effective osmoticant, which has a permeability in PC lipid bilayers of 4×10^{-6} cm/s (Finkelstein, 1976). The smallest pressures are obtained with the most permeant osmoticants, formamide and ethylene glycol, having P_d's in lipid bilayers of $\sim 10^{-4}$.[5]

[5] Note that even for the most permeant osmoticants considered here, the movement of solute is limited by the bilayer and not the unstirred layer. The lower pressures resulting from formamide and ethylene glycol are due to leakage across the contact region and are not due to dissipation of the osmotic gradient across the unstirred layer.

Although the differences in pressures generated by solutes of different bilayer permeability depend on the vesicle radius and the density of channels (Table I), the general order of effectiveness, KCl > urea > formamide ≥ ethylene glycol, is the same. The loss of the permeant osmoticants from the vesicle by leakage through the contact region results in a lower $c_{p,v}$, and therefore a lower ΔP. This can be shown by setting the bilayer permeability coefficients of the nonelectrolytic osmoticants in the contact region, ω_1, to zero, thereby preventing the efflux of all solutes from the vesicle. In this case, the ΔP obtained with any nonelectrolytic osmoticant equals that obtained with KCl. Furthermore, if the bilayer permeability coefficients in the noncontact region, ω_2, are also set equal to zero (in addition to $\omega_1 = 0$), then the pressures are the same as those obtained with setting only $\omega_1 = 0$. Therefore, the osmoticants having larger bilayer permeabilities produce low pressures because they leak out of the vesicle through the region of contact.

TABLE I

Steady-State ΔP for the Permeant Initial Solute–Large Channel Model

Osmoticant	$r = 0.1$ μm	$r = 1.0$ μm
	atm	
KCl	0.597	0.905
Urea	0.593	0.341
Formamide	0.436	0.023
Ethylene glycol	0.416	0.019

Steady-state intravesicular hydrostatic pressures resulting from the permeant initial solute–large channel model (case II) with a 200-mosmol gradient (*cis*) of the indicated osmoticant. The "standard" vesicle is used in the model: 20% of the vesicle's surface area in contact with the planar membrane; one porin channel modeled as a water-filled pipe is placed in the noncontact region. The freely permeating initial solute 100 mM KCl is present everywhere. The ω's and L's for the lipid bilayer were calculated from the P_d's for nonelectrolytes and the P_f of water, which were taken from Finkelstein, 1976. As in all examples, $\omega_1/L_1 = \omega_2/L_2$. Channel permeabilities to solute and water are given in the Appendix. The reflection coefficients of both the osmoticant and KCl are taken as 0.1.

Case III: Impermeant Solutes Inside and Outside the Vesicle

We now consider the situation in which the channels present in the vesicle membrane are permeable to the osmoticant but not to the original contents of the vesicle nor to that of the bathing medium. This mimicks experiments in which the membrane-impermeant fluorescent dye calcein was contained in the vesicle, the two compartments contained sucrose, and nystatin was the vesicular channel (Niles and Cohen, 1987; Cohen et al., 1989).

The osmoticant's molecularity is λ and its reflection coefficient within the channels is σ (subscripts for λ and σ are not used because the bathing solute is impermeant; see Fig. 6). Note that different species of impermeants are allowed in each compartment. To simplify matters, we assume that the membrane-impermeant solute is osmotically balanced in the *cis* and *trans* compartments, and $\lambda = 1$ for both, so that $c_{s,1} = c_{s,2}$. Initially and at steady state $c_{s,v} = c_{s,2}$ because at both times the volume of the vesicle is the same (and equal to V_0) and these species are impermeant. The

equations for the water and solute flux are

$$J_v = L_1[RT(c_{s,v} + \lambda c_{p,v} - c_{s,1}) - \Delta P] + L_2[RT(c_{s,v} - c_{s,2} + \lambda c_{p,v} - \lambda c_{p,2}) - \Delta P] + L_p\{RT[c_{s,v} - c_{s,2} + \sigma\lambda(c_{p,v} - c_{p,2})] - \Delta P\}, \quad (10)$$

$$J_p = -\omega_1 RTc_{p,v} + \omega_2 RT(c_{p,2} - c_{p,v}) + \omega_p RT(c_{p,2} - c_{p,v}) + (1/2)(1 - \sigma)(c_{p,2} + c_{p,v})L_p\{RT[c_{s,v} - c_{s,2} + \sigma\lambda(c_{p,v} - c_{p,2})] - \Delta P\}. \quad (11)$$

At steady state, $J_v = J_p = 0$ and $c_{s,1} = c_{s,v} = c_{s,2}$, and Eqs. 10 and 11 simplify to

$$J_v = 0 = RT\lambda[(L_1 + L_2 + \sigma L_p)c_{p,v} - (L_2 + \sigma L_p)c_{p,2}] - (L_1 + L_2 + L_p)\Delta P \quad (12)$$

and

$$J_p = 0 = RT[(\omega_2 + \omega_p)c_{p,2} - (\omega_1 + \omega_2 + \omega_p)c_{p,v}] + (1/2)(1 - \sigma) \cdot (c_{p,2} + c_{p,v})L_p[RT\sigma\lambda(c_{p,v} - c_{p,2}) - \Delta P]. \quad (13)$$

Solving Eq. 12 for $c_{p,v}$ and substituting into Eq. 13 yields a quadratic equation for the steady-state ΔP of the form $A(\Delta P)^2 + B(\Delta P) + C = 0$, where

$$A = (1/2)(1 - \sigma)L_p b(RT\sigma\lambda b - 1),$$

$$B = (1 - \sigma)L_p c_{p,2}[RT\sigma\lambda ab - (1/2)(1 + a)] - RTb(\omega_1 + \omega_2 + \omega_p),$$

$$C = RT[(1 - a)(\omega_2 + \omega_p) - a\omega_1]c_{p,2} + (1/2)(1 - \sigma)\sigma\lambda L_p RT(a^2 - 1)c_{p,2}^2,$$

$$a = \frac{L_2 + \sigma L_p}{L_1 + L_2 + \sigma L_p},$$

$$b = \left(\frac{1}{\lambda RT}\right)\frac{L_1 + L_2 + L_p}{L_1 + L_2 + \sigma L_p},$$

and

$$c_{p,v} = a \cdot c_{p,2} + b \cdot \Delta P. \quad (14)$$

The final equation clearly reveals the direct relation between the steady-state ΔP and $c_{p,v}$. Solution of the quadratic equation yields the value of the steady-state ΔP. We used this solution to determine how ΔP is affected by the wide collection of independent variables in this model, including the hydraulic and solute permeabilities of the channels, the water and solute permeabilities of bare bilayer, the channel density in the noncontact region, the concentration of the osmoticant in compartment 2, and the reflection coefficient. These parameters were explored over the domains most likely to be encountered in experiments.

To make comparisons convenient, we use the following conditions to define the "standard" vesicle. The vesicle is 1 μm in radius and has 20% of its surface area in contact with the planar membrane, and at least one channel is present in the non-

contact region of the vesicle membrane. Pressures are generated by adding 200 mosmol of an osmoticant to compartment 2.

The Hydraulic Permeability of Channels and Lipid Membrane

The steady-state ΔP is affected by the water permeabilities of both the vesicle membrane and the channels. Since formation of nystatin channels requires sterol in the membrane, we must consider the effects of sterol on steady-state pressures. The P_f of lipid membranes, in addition to the solute's P_d, is decreased by sterols (Finkelstein, 1976). To isolate the effect of a decreased bilayer P_f on the steady-state ΔP, we calculate ΔP for two vesicles, one containing sterol in its bilayer and the other without sterol. Both vesicles contain 100 porin channels with L_p estimated from Poisseuille's law (see Appendix). To obviate the effect of sterol on the solute P_d, we chose 100 mM KCl as the osmoticant, since its $\omega_1 = 0$ (ω_p is estimated from the

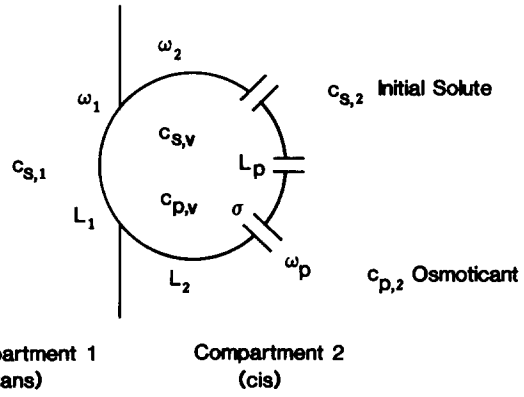

FIGURE 6. Case III. Hyperosmotic swelling of a vesicle with channel- and bilayer-impermeant solutes present both inside and outside the vesicle. The initial solutes, which are impermeant through both the channel and the bilayer, and which need not be the same species, are present at $c_{s,1}$ in compartment 1, $c_{s,v}$ inside the vesicle, and $c_{s,2}$ in compartment 2. Initially and at steady state, $c_{s,1} = c_{s,v} = c_{s,2}$. The experiment is started by adding a channel-permeating and, possibly, bilayer-permeating osmoticant to compartment 2. The osmoticant concentration in compartment 2 is $c_{p,2}$ and in the vesicle it is $c_{p,v}$. Its solute permeability coefficient through the channels is ω_p, and its reflection coefficient in the channels is σ. The hydraulic permeability coefficient of the channels is L_p. As in Case II, at steady state an intravesicular ΔP develops that forces water out the vesicle. This ΔP-driven water efflux balances the osmotic influx of water into the vesicle through the contact region.

conductance of the porin channel, and its σ is set equal to 0.1, see Appendix). Under these conditions, a ΔP of 0.604 atm is produced in the absence of sterol and 0.283 atm in its presence. This smaller ΔP is a direct consequence of decreasing the hydraulic permeability of the contact region (L_1) with sterol. The sterol decreases the influx of water for a given osmotic gradient across the contact region. This smaller influx requires a smaller efflux of water at steady state, and, therefore, the vesicle develops a smaller ΔP.

One can view the vesicle as a bag. For the same steady-state flows, a tight bag holds a larger pressure than a leaky one. As expected from this analogy, a large L_p produces a small ΔP. To illustrate, we again use 100 mM KCl as the osmoticant with 100 porin channels in the vesicle membrane; ω_p to KCl is estimated from the con-

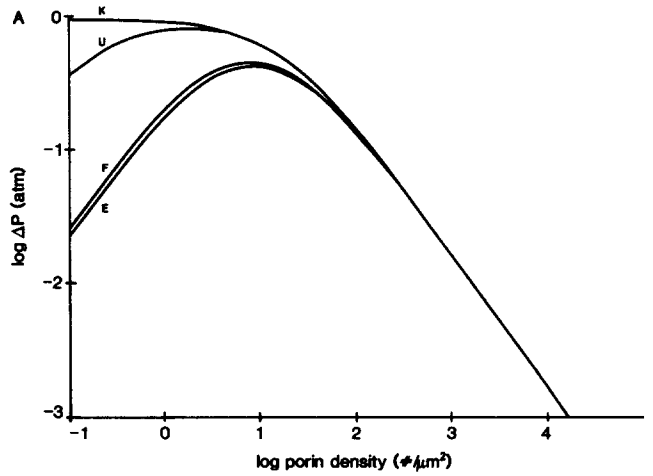
A
K
U
F
E
log ΔP (atm)
0
-1
-2
-3
-1
0
1
2
3
4
log porin density (#/μm²)

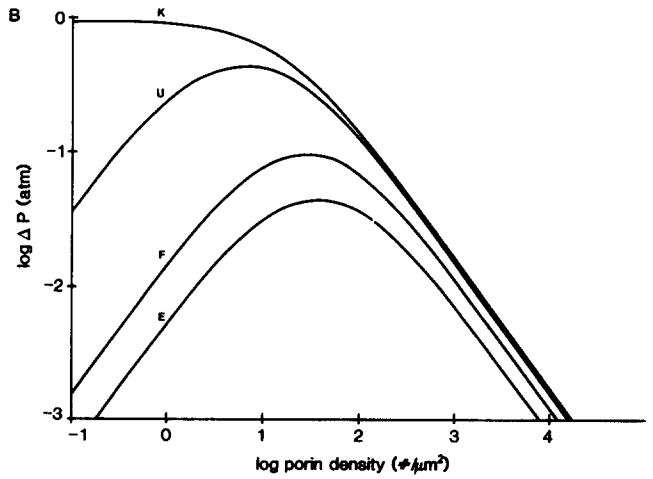
B
K
U
F
E
log Δ P (atm)
0
-1
-2
-3
-1
0
1
2
3
4
log porin density (#/μm²)

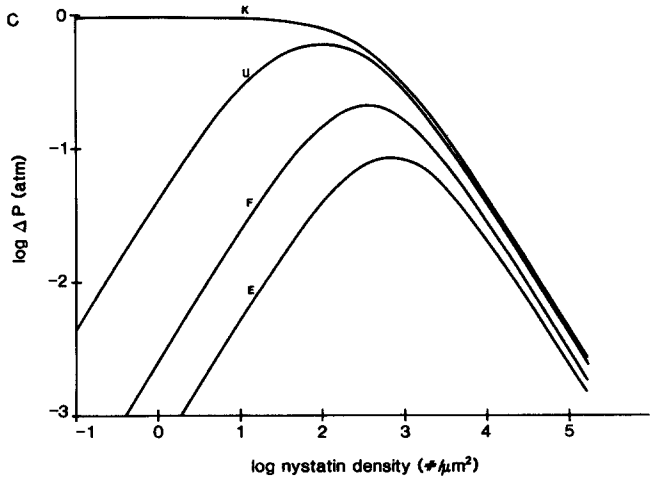
C
K
U
F
E
log Δ P (atm)
0
-1
-2
-3
-1
0
1
2
3
4
5
log nystatin density (#/μm²)

ductance of the porin channel and the reflection coefficient set equal to 0.1 (see Appendix). With the L_p of porin estimated from Poisseuille's law ΔP is 0.604 atm, as given above. Substituting the L_p measured for nystatin (see Appendix) in for the Poisseuille guess of L_p (porin), without altering any other parameters, yields a higher ΔP of 0.985 atm. At steady state, the rates of osmotically induced water influx are the same in the two cases because the $c_{p,v}$'s are the same; the larger L_p allows a high rate of water efflux with a smaller ΔP. (Note that the net influx of water across the contact region is larger for the higher L_p vesicle.)

The Density of Channels in the Noncontact Region

ΔP is ultimately determined by the density of channels in the vesicle. The channels are the principal routes through which osmoticant enters and water leaves the vesicle; their density sets both ω_p and L_p. We illustrate how ΔP is influenced by the interaction between the permeation properties of the single channel and the density of those channels by using different estimates of ω_p. The results are shown in Fig. 7, where ΔP is plotted as a function of the density of porin (Fig. 7, *A* and *B*) and nystatin channels (Fig. 7 *C*) for four different osmoticants under standard conditions. In Fig. 7 *A*, the porin channel was modeled as a water-filled pipe 5.8 Å in radius and 5 nm in length; L_p was estimated from Poisseuille's law and ω_p from free diffusion (see Appendix). In Fig. 7 *B*, the free-diffusion ω_p was corrected for steric hindrance of solute passage through the pore by a Renkin coefficient (see Appen-

FIGURE 7. (*Opposite*) ΔP as a function of porin (*A* and *B*) and nystatin (*C*) channel densities for case III, where channel-impermeant solutes are present inside and outside the vesicle. Steady-state ΔP's are plotted against the logarithm of channel density in the noncontact region of the vesicle (number of channels/μm^2). The following osmoticants were used to make a 200 mosmol gradient (compartment 2 hyperosmotic): KCl (*K*), urea (*U*), formamide (*F*), and ethylene glycol (*E*). The vesicle radius was 1 μm and 20% of its surface area was in the contact region. (*A*) ω_p (porin) for nonelectrolytes estimated by modeling the channel as a water-filled pipe (see Appendix). (*B*) ω_p (porin) for nonelectrolytes estimated by correction of the ω_p in *A* for steric hindrance (see Appendix). (*C*) ω_p (nystatin) estimated from permeability constants (*U, F, E*) measured for double-sided nystatin channels in planar bilayers (see Appendix). In *A–C*, bilayer permeabilities to KCl (ω_1 and ω_2) were set equal to 0. In *A* and *B*, for urea, ω_1 and ω_2 were the same as in Fig. 5 *B*; for formamide, $\omega_1 = 1.044 \times 10^{-22}$ mol·cm^3/erg·s and $\omega_2 = 4.176 \times 10^{-22}$; for ethylene glycol, $\omega_1 = 8.921 \times 10^{-23}$ and $\omega_2 = 3.568 \times 10^{-22}$. L_1 and L_2 are the same as in Fig. 5 *B*. Membrane permeability coefficients for sterol-containing PC bilayers were used in *C*; for urea, $\omega_1 = 6.184 \times 10^{-25}$ and $\omega_2 = 2.473 \times 10^{-24}$, for formamide, $\omega_1 = 1.592 \times 10^{-23}$ and $\omega_2 = 6.366 \times 10^{-23}$, and for ethylene glycol, $\omega_1 = 1.358 \times 10^{-25}$ and $\omega_2 = 5.434 \times 10^{-23}$. In *C*, $L_1 = 9.799 \times 10^{-21}$ cm^6/erg·s and $L_2 = 3.919 \times 10^{-20}$. In *A–C*, the ω_p for KCl was estimated from the conductance of the porin (*A* and *B*) or double-sided nystatin (*C*) channel (Table AII). In both wide-open and restricted-diffusion porin channels, σ's for all osmoticants are taken as 0.1. In the nystatin channel, σ is taken as 0.99 for KCl, 0.55 for urea, 0.52 for formamide, and 0.67 for ethylene glycol (Holz and Finkelstein, 1970). With the salt osmoticant ($\omega_1 = 0$), the maximum ΔP is attained with one channel in the noncontact region. For the nonelectrolytes, ΔP increases to a maximum and then decreases as the channel density is increased. The more permeant osmoticants produce ΔP's much smaller than those from urea and KCl at small channel densities.

dix)[6]; the same value of L_p as in Fig. 7 *A* was used. Fig. 7 *C* shows the same relation between ΔP and channel density for nystatin; measured values of L_p, ω_p, and σ for nystatin channels were used (Holz and Finkelstein, 1970), and the lipid membrane permeabilities were those measured with sterol in the membrane (Finkelstein, 1976). In all cases, permeabilities of KCl were estimated from the conductances of the channels (see Appendix).

As shown in Fig. 7, the steady-state ΔP increases with channel density until a maximum ΔP is reached. Thereafter ΔP decreases as the channel density increases. Both the maximum ΔP and the corresponding channel density are dependent on ω_p and ω_1, and hence, vary with osmoticant. The values of ΔP for all osmoticants, however, converge to a monotonically decreasing curve with a slope characteristic of the channel, once the channel density is greater than optimum. ΔP is dominated by L_p in this range of large channel densities. ΔP is dissipated by driving water from the vesicle through the numerous channels. With lower channel densities, ΔP is determined by ω_p and ω_1.

The balance of the solute entering the vesicle through the channels and exiting the vesicle via the contact region determines the maximum ΔP (ΔP_{max}) and the channel density required to achieve it. This is most clearly seen in the case of KCl, with its $\omega_1 = 0$. One porin or nystatin channel in the noncontact region (0.1 channels/μm^2) is sufficient for ΔP_{max}. ΔP_{max} is slightly greater with nystatin (Fig. 7 *C*) because its L_p is less than porin's. Nevertheless, the maximum pressures are quite close despite the three orders of magnitude disparity between the values of ω_p for the two channels for KCl. A single channel of either type allows enough KCl to enter the vesicle to achieve an appreciable steady-state ΔP. Since the KCl is impermeant through the contact region, the osmoticant is not lost by this route and $c_{p,v}$ approaches $c_{p,2}$.

For the bilayer-permeant osmoticants, the maximum pressures and the corresponding channel densities show a direct relation to ω_1. The leakiest nonelectrolytes, formamide and ethylene glycol, require larger channel densities than the less permeant urea to attain maximum pressures. Moreover, the magnitude of the maximum ΔP is less for a solute lost through the contact region than for one less permeant.[7] The permeant solutes exit the vesicle through the contact region, resulting in a lower $c_{p,v}$, which directly produces a diminished ΔP. The influx of solute through the channel is able to compensate the loss of osmoticant, provided that entry exceeds the rate of exit. Hence, ΔP, increases with channel density until the solute influx is able to maintain $c_{p,v}$ near $c_{p,2}$ despite leakage. If the osmoticant has a large ω_1, a greater channel density is necessary to offset the leakage. ΔP_{max} is less for the leakiest solutes because these higher channel densities result in a larger L_p.

The ΔP maxima are smaller and the corresponding channel densities are larger

[6] The reflection coefficient of the osmoticant in the channel (σ) is not corrected similarly (i.e., increased due to steric hindrance), but was fixed at 0.1 for both free- and restricted-diffusion estimates of ω_p. As will be seen, the steady-state ΔP is relatively insensitive to the value of σ with porin as the channel and with the relatively small nonelectrolytes we use.

[7] Formamide generates somewhat larger pressures than ethylene glycol, despite its larger P_d (P_d for formamide through PC bilayers is 1.03×10^{-4} cm/s, whereas the P_d for ethylene glycol is 8.8×10^{-5} cm/s, Finkelstein, 1976). This arises because formamide has a smaller molecular radius than ethylene glycol and hence, has a greater single-channel ω_p.

when the magnitude of the single-channel ω_p is decreased by restricting diffusion through the channel. For example, ΔP_{max} for urea of 0.79 atm occurs at a porin density of 2 channels/μm^2 (20 channels in the noncontact region of a 1-μm-radius vesicle) when porin is modeled as an open pipe (Fig. 7 *A*). Restricting diffusion through this pipe (Fig. 7 *B*) decreases it to 0.44 atm and moves it to 7 channels/μm^2 (73 channels). This effect is much greater for solutes with higher permeabilities through the contact region. With ethylene glycol, ΔP_{max} is 0.42 atm at 10 open-pipe porin channels/μm^2 (101 channels) and is 0.04 atm with 40 restricted-pipe porin channels/μm^2 (398 channels). As the permeant solute leaks out of the vesicle, decreasing $c_{p,v}$ and ΔP, the bigger channel is able to replenish the lost solute faster than the smaller one and to maintain $c_{p,v}$ near $c_{p,2}$. Hence, more smaller channels are needed to offset the leakage of solute, and ΔP is maximized at a higher density. At the optimum density, the ΔP_{max} is smaller with restricted porin channels than with wide-open porin channels, because the total L_p is greater with the larger number of restricted channels.

Nystatin channels (Fig. 7 *C*) yield similar results to restricted diffusion through porin channels. The smaller radius of the nystatin channel causes discrimination between the osmoticants on the basis of their sizes. A very bilayer-permeant, yet somewhat bulky solute such as ethylene glycol (molecular radius, 2.8 Å) generates a small ΔP_{max} (0.08 atm with 7,157 nystatin channels/μm^2). The nystatin channels hinder the entry of ethylene glycol, and the solute that does enter tends to leak out through the contact region, keeping $c_{p,v}$ and ΔP low. This sieving effect enhances the differences between the permeant osmoticants for both the maximum pressures and the corresponding channel densities.

ΔP_{max} is attained with about one or two orders of magnitude more nystatin channels than porin channels of either type. For illustration, ΔP_{max} with 200 mM urea requires 100 nystatin channels/μm^2 (1,000 channels). This ΔP_{max} is larger than the one obtained with restricted porin channels but smaller than that of porin channels modeled as an open pipe. Restricted porin channels differ from nystatin channels because their L_p is 100 times greater than nystatin's (i.e., the L_p of a vesicle with 7 restricted porin channels/μm^2 is seven times that of one with 100 nystatin channels/μm^2).

While the ω_p of a nystatin channel for urea is about 1,000 times less than that of a wide-open porin channel, ΔP_{max} occurs with only 50 times more nystatin channels than porin channels (see above). This comes about for two reasons. First, the sterol in the contact region decreases ω_1 by a factor of about five (Finkelstein, 1976). Therefore, only 200 times more nystatin than porin channels provide the solute influx needed to compensate for the diminished efflux of solute. Second, the sterol also decreases L_1 by a factor of about four, so that steady state is reached with L_p (the number of channels) decreased by an additional factor of four. Nystatin's ΔP_{max} is decreased with respect to that of porin modeled as an open pipe because of the nystatin channel's smaller single-channel ω_p and the smaller ω_1 and L_1 due to the presence of sterol in the contact region. Although the L_p of the vesicle containing 100 nystatin channels/μm^2 is one-half that of a vesicle containing 2 porin channels/μm^2, the lower ΔP_{max} occurs because the vesicle can accommodate a solute influx rate that is only one-fourth of that of the porin-containing vesicle. The nystatin-

containing vesicle maximizes ΔP by keeping L_p small at the expense of solute influx, which results in a decreased ΔP_{max} for nystatin channels with respect to open-pipe porin channels.

Vesicle Radius at a Fixed Channel Density

ΔP is invariant to changes in vesicle radius (r) at constant channel density and contact area fraction (f). This is shown in Fig. 8, where ΔP is plotted as a function of vesicle radius from 50 nm to 10 μm. The area of contact was fixed at 20%, and the

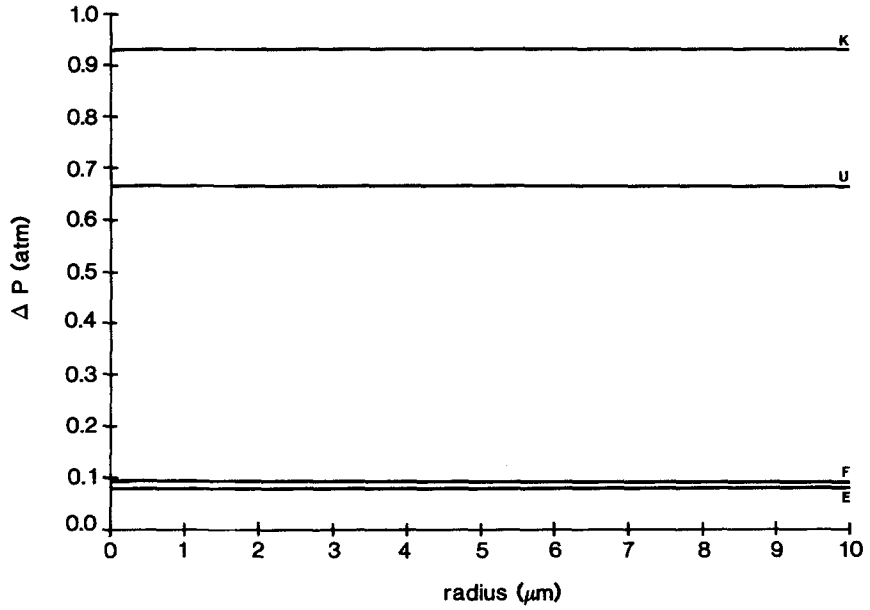

FIGURE 8. ΔP as a function of vesicle radius at constant channel density. Steady-state intravesicular hydrostatic pressure is plotted against vesicle radius, with the density of porin channels in the noncontact region fixed at 1 channel/$3.2 \cdot \pi$ μm^2 (80% of vesicle area in noncontact region). ω_p and L_p for the porin channels were calculated according to the water-filled pipe model (see Appendix). Plots are shown for a 200 mosmol gradient (compartment 2 hyperosmotic) of the following osmoticants: KCl (K), urea (U), formamide (F), and ethylene glycol (E). ΔP is invariant to vesicle radius when the density of channels is held constant. This indicates that ΔP is determined by the relative size of osmoticant influx through the channels compared to its efflux through the contact region.

density of channels in the contact region was fixed at 0.1 porin channels/μm^2 (uncorrected pipe model). (We note that there is less than one porin channel in the noncontact region for $r < 0.91$ μm at this density. Physical realization of this spatial regime would require a channel with ω_p and L_p proportionally decreased.) The ΔP developed by 200 mosmol of the indicated osmoticant is independent of radius, but dependent on the osmoticant's ω_1. This occurs because as r increases under these conditions, ω_1 and $(\omega_p + \omega_2)$ both increase in proportion to the vesicular area, and the rates of solute influx (through the channels and the bilayer in the noncontact

region) and efflux (through the contact region and solvent drag through the channels) also increase in the same proportion. The hydraulic permeabilities similarly scale such that osmotic influx through the contact region increases in proportion to the osmotic and ΔP-driven efflux of water. This results in the same $c_{p,v}$ and hence the same ΔP at all radii. The lower ΔP for leaky solutes is due to leakage of the solute out through the contact region, which lowers $c_{p,v}$, which in turn causes the lower ΔP.

Effect of Osmoticant Concentration

Because the precise variation of ΔP with channel density depends on the type of osmoticant (Fig. 7), we evaluate the dependence of ΔP on the osmoticant concentration in two ways. In the first, the channel density yielding the maximum ΔP is used for each osmoticant. This reveals the effectiveness of each osmoticant under the most favorable combination of ω_1 and ω_p. In the second, the channel density is fixed at an arbitrary value. This resembles experiments where the channel density in the vesicles is distributed around a fixed mean.

The dependence of the maximum ΔP on osmoticant concentration is shown in Fig. 9, *A* and *B*. In these plots, the solute osmolality given on the abscissa is the excess osmolality of the solute in compartment 2 over that in compartment 1. The set of curves in Fig. 9 *A* is obtained with the porin channel modeled as a pipe in a sterol-free bilayer. Measured values of ω_p and L_p for nystatin and bilayer permeabilities for sterol-containing bilayers are used in Fig. 9 *B*. In all cases, KCl results in the largest ΔPs because it has the lowest ω_1 (ΔP obtained with 500 mM KCl is greater than ΔP with 1,000 mM urea). The next most effective osmoticant is urea, which has the next lowest ω_1. Formamide and ethylene glycol produce the lowest, and for porin modeled as a pipe, comparable ΔPs. In all cases, the order of maximum ΔP follows the general trend of ω_1: KCl > urea > formamide ≥ ethylene glycol (see footnote 6).

These differences between the osmoticants are most pronounced when a fixed (low) channel density is used, as is the case in experiments with reconstituted channels. This is shown in Fig. 9 *C* where ΔP is plotted as a function of osmoticant concentration with the channel density fixed at one porin channel in the noncontact region of a standard, 1-μm-radius vesicle. The order of osmoticants in the magnitudes of ΔPs they produce is the same as when an optimum channel density is used. The differences in ΔP are larger, however, because the channel densities are not adjusted to compensate for the leakage of the osmoticant out of the vesicle through the contact region.

Interactions of Solute and Water Fluxes in the Channel

ΔP depends on the degree of coupling between solute and water fluxes within small channels, but not within large channels for the solutes that we are considering. In Fig. 10, the relation between ΔP and nystatin channel density is plotted for 1,000 mM KCl at two values of the reflection coefficient, σ, 0.01 and 0.99 (σ for KCl is actually 0.99). In general, ΔP is greater at larger values of σ (decreased interaction between solute and water in the channels). Moreover, the σ of an osmoticant has a large effect on the relation between ΔP and channel density; ΔP attains greater val-

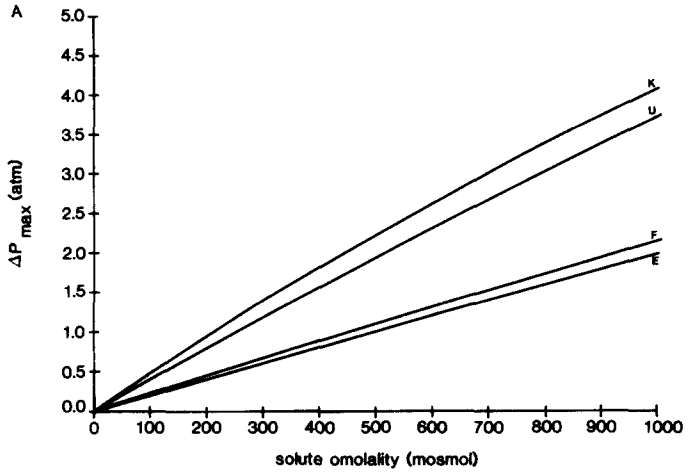
A
5.0
4.5
4.0
3.5
3.0
2.5
2.0
1.5
1.0
0.5
0.0
ΔP max (atm)
K
U
F
E
0
100
200
300
400
500
600
700
800
900
1000
solute omolality (mosmol)

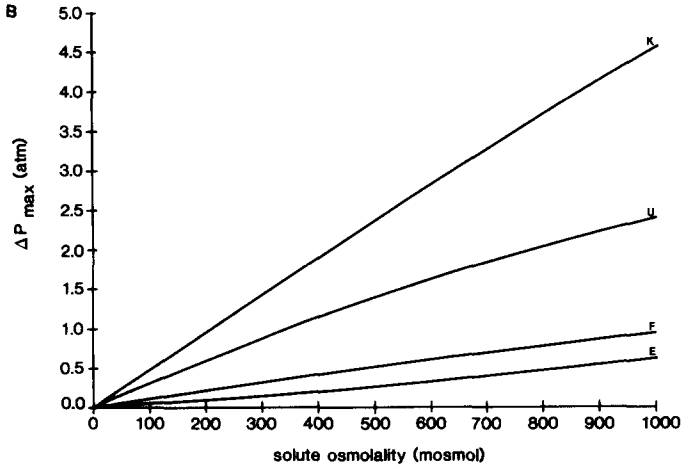
B
5.0
4.5
4.0
3.5
3.0
2.5
2.0
1.5
1.0
0.5
0.0
ΔP max (atm)
K
U
F
E
0
100
200
300
400
500
600
700
800
900
1000
solute osmolality (mosmol)

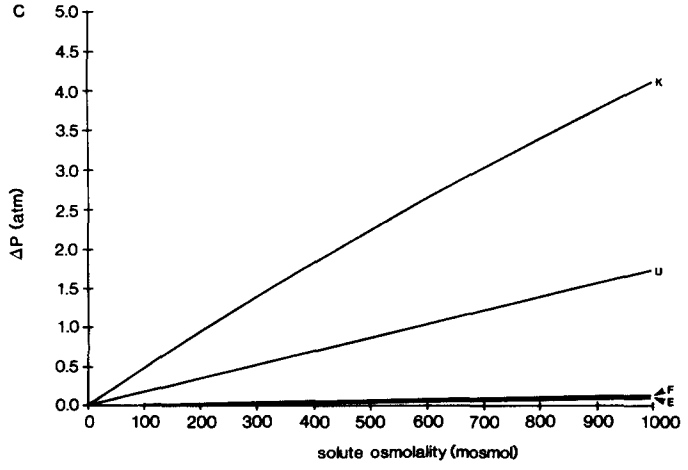
C
5.0
4.5
4.0
3.5
3.0
2.5
2.0
1.5
1.0
0.5
0.0
ΔP (atm)
K
U
F
E
0
100
200
300
400
500
600
700
800
900
1000
solute osmolality (mosmol)

ues at low channel densities when σ is near 1. As the channel density is increased, ΔP decreases more steeply when σ is large. This arises from the variation of ΔP with L_p; $d(\Delta P)/dL_p$ is approximately proportional to σ (see Eq. 14). As the channel density is made very large, differences between the ΔPs at different σ's become very small. Thus, strong coupling between solute and water fluxes within the channel (σ near 0) results in a lower steady-state ΔP.

σ affects ΔP to the greatest extent at high concentrations of osmoticant. With 1,000 nystatin channels in a standard vesicle, σ's of 0.01 and 0.99 produce negligible differences when 100 mM urea is used (0.3177 and 0.3178 atm, respectively). In contrast, 1,000 mM urea produces a 30% difference, with $\Delta P = 3.1$ at $\sigma = 0.99$ and 2.2 atm at $\sigma = 0.01$. The concentration dependence arises from the convective term in the expression for solute influx (Eq. 11). This term, $(1 - \sigma)\bar{c} \cdot J_v$, varies directly with the average concentration of the solute within the channel ($\bar{c}$) rather than with the difference in concentration between the two ends of the channel. Thus, the amount of solute carried along with any pressure-driven flow of water through the channel is proportional to its concentration.

σ exerts the greatest influence on ΔP when the single-channel permeabilities are small, e.g., nystatin. With a single porin channel modeled as a pipe, decreasing σ from 0.99 to 0.01 has a small effect on the ΔP generated by 1,000 mM urea (1.78 vs. 1.74 atm, respectively). When diffusion through this pipe is restricted (see Appendix), this difference between the two σ's is increased (0.176 vs. 0.156 atm).[8]

[8] Whereas ω_p of the porin channel was corrected with the Renkin coefficient, σ was not corrected (see footnote 6). Instead, σ was varied over a large range of possible values when ω_p was fixed, and, conversely, ω_p was varied when σ was fixed. In the most realistic simulation of solute permeation through a water-filled channel, σ would be increased as ω_p is decreased, since less permeant solutes do not interact to as great an extent with the waterflow through the channel and, hence have σ's nearer to 1 than more permeant solutes. Since ΔP is not affected by σ until ω_p is very small (e.g., a nystatin channel), we did not vary ω_p and σ simultaneously for porin. Furthermore, a correction to σ based on molecular size would be based on ad hoc assumptions in addition to those used to correct ω_p.

FIGURE 9. (*Opposite*) ΔP as a function of osmoticant osmolality. ΔP is plotted against the excess osmolality of osmoticant in compartment 2 over compartment 1 for the four osmoticants: KCl (*K*), urea (*U*), formamide (*F*), and ethylene glycol (*E*). Effects on ΔP of channel density and methods of estimating ω_p are shown. ω's and L's for lipid bilayer are the same as in Fig. 7, as are the σ's. (*A*) Porin channel modeled as a pipe (see Appendix). The following channel densities were used that result in the maximum ΔP (ΔP_{max}) for each osmoticant: KCl, $0.1/\mu m^2$ (1 channel); urea, $2/\mu m^2$ (20 channels); formamide, $8/\mu m^2$ (80 channels); ethylene glycol, $10/\mu m^2$ (100 channels). (*B*) Nystatin channel. The channel density is that corresponding to the maximum ΔP (ΔP_{max}) for each osmoticant: KCl, $0.1/\mu m^2$ (1 channel); urea, $100/\mu m^2$ (1,000 channels); formamide, $335/\mu m^2$ (3,368 channels); ethylene glycol, $712/\mu m^2$ (7,157 channels) (*C*) The channel density is fixed at one porin channel (modeled as a pipe) in the noncontact region. For all three panels, the vesicle is 1 μm in radius and has 20% of its area in contact with the planar membrane. The relative order of potency of these osmoticants, KCl > urea > formamide $\geq$ ethylene glycol, is the same in all three cases, even when the channel densities are optimized. This indicates that the effectiveness of an osmoticant in supporting fusion depends on its permeability through the lipid bilayer of the contact region.

Nevertheless, the greatest differences are obtained with nystatin, which has the smallest ω_p's used, and the greatest extent of these differences amounts to about an order of magnitude (Fig. 10).

That coupling of solute and water fluxes influences the steady-state ΔP only when ω_p is small, is a consequence of the nature of solute flux as seen in Eq. 11, which consists of both diffusive and convective terms. At steady state, the ΔP-driven water flux out of the vesicle through the channel and bilayer balances the influx of water

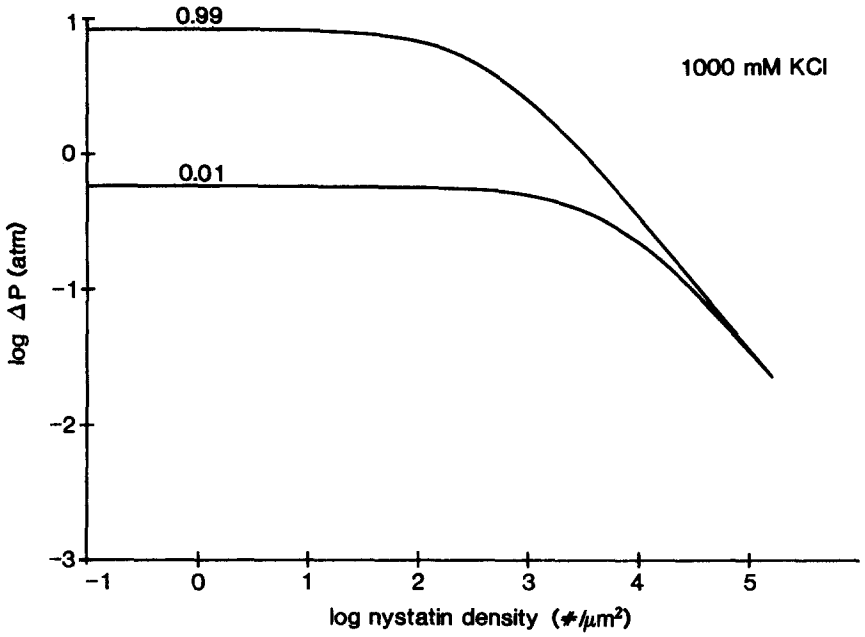

FIGURE 10. Effect on steady-state ΔP of the osmoticant's reflection coefficient (σ) inside the channel. ΔP is plotted as a function of nystatin channel density in the noncontact region of the vesicle. The vesicle is 1 μm in radius, has 20% of its area in the contact region, and is swollen with 1,000 mM KCl in compartment 2. The σ of KCl inside the nystatin channel is varied between 0.99 (top curve) and 0.01 (bottom). ω's and L's of the lipid bilayer are as in Fig. 5 *B*. The greatest degree of interaction between KCl and water flows within the channel occurs with the smallest value of σ used (0.01), and produces a ΔP about one-tenth that in the absence of coupling. This results from the ΔP-driven water efflux through the channel sweeping KCl out of the vesicle, which decreases $c_{p,v}$. As σ increases, the extent of interaction between KCl and water decreases, the ΔP-driven efflux of water has less effect on $c_{p,v}$, and ΔP is increased.

driven by the osmotic gradient across the contact region. Thus, any coupling between solute and water fluxes within the channel results in the efflux of solute from the vesicle. When σ is near 0 (flux coupling is very tight), the efflux of water through the channel drags solute with it. When ω_p is small, coupling effectively lowers $c_{p,v}$ because the diffusive influx of solute through the channel is insufficient to compensate for the loss of solute. This results in a lowered ΔP. When σ is near 1, so that flows of solute and water are independent, the water efflux through the chan-

nel does not diminish $c_{p,v}$, and ΔP remains large. If ω_p is large, then the influx of solute by diffusion through the channel replenishes that which is lost by coupling to the water efflux.

Finally, while ΔP is much less dependent on σ for channels with large ω_p, it should be appreciated that significant osmoticant is swept along with the pressure-driven water efflux. For large channels the water-coupled solute efflux is balanced by consequent diffusive influx. The convective efflux and diffusive influx of solute therefore constitute a futile cycle for large channels. Of course, in the steady state, there is no net flux of solute through the channel if the osmoticant is bilayer-impermeant and there is a net influx for a bilayer-permeant osmoticant.

Case IV: Isosmotic Substitution of Permeant for Impermeant Solutes

In the final case, an impermeant solute bathing the vesicle is replaced with an isosmotic quantity of a permeant solute. This case is isomorphic with experiments in

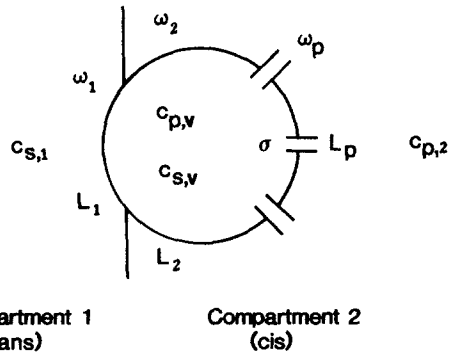

FIGURE 11. Case IV. Isosmotic swelling of a vesicle with an impermeant solute trapped inside. The initial solute, which is impermeant through both lipid bilayer and the channels, is present in compartments 1 and 2 at $c_{s,1}$ and in the vesicle at $c_{s,v}$ ($c_{s,1} = c_{s,v}$). Swelling is started by replacing all of the impermeant solute in compartment 2 with a solute that is permeant through both lipid bilayer and the channels. The concentration of permeant solute in compartment 2 is $c_{p,2}$ and inside the vesicle is $c_{p,v}$ ($c_{p,2} = c_{s,v}$). This method of swelling produces the largest ΔP of any of the methods considered if $c_{p,v} = c_{p,2}$, in which case $\Delta P = RTc_{s,v}$.

which porin-impermeant solutes (stachyose) bathing porin-containing vesicles (with stachyose inside) were replaced with an isosmotic quantity of permeant solutes (Cohen et al., 1982; Akabas et al., 1984; Cohen et al., 1989). In this case, water flux into the vesicle is driven by two separate components of the total osmotic force. The first component results from the channel-impermeant solute trapped inside the vesicle. The lower σ of the permeant solute outside the vesicle in compartment 2 causes that solute to exert less of an osmotic driving force than does the impermeant solute trapped inside the vesicle, thus leading to osmotic flow of water into the vesicle. The second component arises from the diffusion of the permeant solute through the channel into the vesicle, which creates an osmotic gradient between the vesicle and compartment 2 that pulls water into the vesicle.

The situation is illustrated in Fig. 11. The vesicle with channels embedded in its membrane is initially bathed in a channel-impermeant buffer at concentration $c_{s,1}$ in compartment 1, $c_{s,v}$ inside the vesicle, and $c_{s,2}$ in compartment 2, where $c_{s,1} = c_{s,v} =$

$c_{s,2}$. At $t = 0$, the impermeant solute in compartment 2 is replaced with a channel-permeant solute at a concentration $c_{p,2}$, where $c_{s,2} = c_{p,2}$. For simplicity's sake, we let the two different solutes have the same λ's. The original, channel-impermeant solute is also impermeant through lipid bilayer. The permeant solute permeates lipid bilayer with permeability coefficients ω_1 in the contact region and ω_2 in the noncontact region. ω_p is the solute permeability coefficient of the channel and σ is its reflection coefficient. Thus, the equation for water flux is

$$\begin{aligned} J_v = {} & L_1[RT(c_{s,v} + c_{p,v} - c_{s,1}) - \Delta P] \\ & + L_2[RT(c_{s,v} + c_{p,v} - c_{p,2}) - \Delta P] \\ & + L_p\{RT[c_{s,v} + \sigma(c_{p,v} - c_{p,2})] - \Delta P\}, \end{aligned}$$

and, since $c_{s,1} = c_{s,v} = c_{p,2}$,

$$J_v = RT(L_1 + L_2 + \sigma L_p)c_{p,v} + RT \cdot L_p(1 - \sigma)c_{s,v} - (L_1 + L_2 + L_p)\Delta P \qquad (15)$$

where $c_{p,v}$ is the concentration of permeant solute inside the vesicle. The expression for solute flux is given by:

$$\begin{aligned} J_p = {} & -\omega_1 RTc_{p,v} + \omega_2 RT(c_{p,2} - c_{p,v}) + \omega_p RT(c_{p,2} - c_{p,v}) \\ & + (1/2)(1 - \sigma)(c_{p,v} + c_{p,2})L_p\{RT[c_{s,v} + \sigma(c_{p,v} - c_{p,2})] - \Delta P\} \end{aligned} \qquad (16)$$

Solving Eqs. 15 and 16 for ΔP at steady state ($J_v = J_p = 0$) yields a quadratic equation of the form, $A(\Delta P)^2 + B \cdot \Delta P + C = 0$, where

$$A = (1/2)(1 - \sigma)L_p b[RT\sigma b - 1]$$

$$B = (1/2)(1 - \sigma)L_p\{RT[1 + 2\sigma a)]b - (1 + a)\}c_{s,v} - RTb(\omega_1 + \omega_2 + \omega_p)$$

$$C = RT[(1 - a)(\omega_2 + \omega_p) - a\omega_1]c_{s,v}$$

$$+ (1/2)(1 - \sigma)L_p RT[1 + (1 - a)\sigma](1 + a)c_{s,v}^2$$

$$a = -(1 - \sigma)\frac{L_p}{L_1 + L_2 + \sigma L_p}$$

$$b = \frac{L_1 + L_2 + L_p}{RT(L_1 + L_2 + \sigma L_p)}$$

and

$$c_{p,v} = a \cdot c_{s,v} + b \cdot \Delta P. \qquad (17)$$

Substitution into Eq. 15, with $J_v = 0$, shows that if $c_{p,v} = c_{p,2}$ (which occurs if $\omega_1 = \omega_2 = 0$), then $\Delta P = RTc_{s,v}$. This is the maximum ΔP that can be expected with this system or any of the cases that we have considered. The most important feature

is that the maximum ΔP depends only on the concentration of the impermeant species trapped inside the vesicle.

This system is able to attain a steady state without the complete dissipation of the concentration gradient of the permeant solute across the vesicle membrane. Steady state is reached when the diffusion-driven flux of solute into the vesicle equals the efflux of solute through the contact region and the water flow into the vesicle through the channel equals the efflux of water through the bilayer into compartments 1 and 2. If ω_1 is not 0, then the vesicle reaches steady state with $c_{p,v} < c_{p,2}$ and $\Delta P < RTc_{s,v}$. Alternatively, when KCl is used as the channel-permeant solute, the vesicle attains equilibrium, because $\omega_1 = 0$. At equilibrium, $c_{p,v} = c_{p,2}$, so that there is no flux of KCl through the vesicle; furthermore, $\Delta P = RTc_{s,v}$, so that there are no steady-state fluxes of water through the vesicle.

The pressures generated by this isosmotic method of swelling are less sensitive to ω_1 than the hyperosmotic swelling methods. This is seen by comparing the ΔP generated by 100 mosmol urea, 2.44 atm, with that resulting from the same amount of formamide, 2.06 atm, in a "standard" vesicle initially containing 100 mosmol of impermeant solute and with one porin channel (pipe) in the noncontact region. This difference between the pressures developed with urea and formamide is less than that observed with the hyperosmotic swelling methods. The basis for this smaller difference is that in isosmotic swelling the vesicle never shrinks, and all solute that enters the vesicle contributes to a hydrostatic pressure. Even permeant solute not entering the vesicle contributes to the ΔP due to its small σ. On the other hand, when osmotic gradients are established across the planar membrane, the vesicle initially shrinks so that a fraction of the osmoticant that enters the vesicle does not contribute to the ΔP, but rather promotes reswelling of the vesicle. With the loss of a leaky solute through the contact region, an even larger fraction of the initial concentration gradient of osmoticant is dissipated in reswelling the vesicle. Also note that for isosmotic swelling, $\Delta P = 0$ only if $c_{p,v} = ac_{s,v}$ (Eq. 17). But as $a < 0$, this is not possible, and zero steady-state pressures are never obtained. For hyperosmotic swelling, however, Eq. 14 shows that $\Delta P = 0$ is possible.

DISCUSSION

We have examined the theoretical basis for the fusion of vesicles to planar membranes by the osmotic swelling of the vesicles. We wanted to determine whether an intravesicular hydrostatic ΔP drives fusion. We knew from experiments that the magnitude of the osmotic gradient necessary for fusion depended on the bilayer permeability of the osmoticant (Cohen et al., 1989). We now understand the underlying basis for this observation; the size of the ΔP generated by osmotic swelling of the vesicle is sensitive to the leakage of the osmoticant out of the vesicle.

In general, the steady-state ΔP is determined by the ω's and L's. These permeability coefficients govern the fluxes of water and solute through the vesicle, which, in turn, ultimately determine $c_{p,v}$ and ΔP. Thus, the magnitude of the ΔP developed by osmotic swelling can be predicted from the permeability properties of both the bilayer (vesicle and planar membrane) and the channels to the osmoticant. As ΔP drives fusion, the model provides the physical basis both for explanations of experi-

mental observations and for methodologies to improve the utility of vesicle fusion with planar membranes.

The Role of Channels

The model predicts the need for open channels in the development of a $\Delta P > 0$. It is likely that vesicles reconstituted with voltage-dependent Na^+ channels do not fuse with planar membranes in the absence of batrachotoxin (BTX), because the channels are closed in its absence. Hartshorne et al. (1985) note this requirement for BTX but have asserted that fusion has occurred in its absence. It may also be, at least in part, the reason that fusion techniques have not been successful for reconstituting the nicotinic acetylcholine receptors into planar membranes without opening the channel. Indeed, reconstitution experiments (using fusion) are aided by open channels in the vesicles. To reconstitute channels into planar membranes, one often establishes the osmotic gradient by making the *trans* compartment hypoosmotic with respect to both the *cis* compartment and the vesicle interior. In this case, ΔP develops without open channels.

For cases II and III, in which the *cis* compartment is made hyperosmotic, the development of a ΔP depends critically on channels, which allow the osmoticant access to the vesicle's interior. Moreover, the ΔP ultimately depends on the solute permeabilities of both the channel and the membrane in the contact region. If ω_p is not sufficiently greater than ω_1, the concentration of solute in the vesicle remains relatively low and the osmotic influx of water into the vesicle through the contact region ($c_{p,v} > c_{s,1}$) is balanced by the osmotic efflux through the noncontact region ($c_{p,2} > c_{p,v}$), without the development of a large ΔP. As channels are added to the noncontact region so that $\omega_p > \omega_1$, the solute influx rate exceeds its efflux rate through the contact region, and $c_{p,v}$ increases. As $c_{p,v}$ approaches $c_{p,2}$, the osmotic contribution to the water efflux into compartment 2 diminishes, while the water flux into the vesicle from compartment 1 increases ($c_{p,v} \gg c_{s,1}$). This greater net influx of water results in the vesicle developing a larger ΔP at steady state. $c_{p,v}$ is often within 1% of $c_{p,2}$ at steady state. In this case, ΔP is the primary force for generating water efflux. Moreover, development of a ΔP is the only way the vesicle can achieve steady state.

As even more channels are placed in the noncontact region, ω_p and L_p increase and the steady-state ΔP decreases. This results from the ΔP-driven efflux of water out of the vesicle through the channels. The vesicle is able to reach steady state with a lower ΔP because of the increased L_p. For channels with a small ω_p, the solvent-coupled solute efflux further lowers ΔP by lowering $c_{p,v}$. For KCl, ω_1 is 0, and the maximum ΔP is attained with one porin or nystatin channel. In the case of the nonelectrolyte osmoticants, for which ω_1 is not 0, several channels are needed before the rate of solute entry exceeds the rate of solute leakage through the contact region. Hence, ΔP increases with channel density until a maximum is reached. Further increases in channel density result in ΔP-driven water and solute effluxes through the channels, which result in lower steady-state values of ΔP and $c_{p,v}$. Differences between the osmoticants become small at these high channel densities because ΔP is dissipated by the large L_p of the many channels. Thus, the optimum channel

has an ω_p large enough to compensate for any osmoticant leakage through the contact region, while having a small L_p to avoid dissipation of any ΔP.

The Time Course of Swelling

When an osmoticant is added, it is misleading to simply divide the process into an initial shrinkage, due to making the outside of the vesicle hyperosmotic, followed by a swelling phase due to the simultaneous entry of osmoticant and water. A small vesicle shrinks very quickly when the surrounding medium is made hyperosmotic, because of the large hydraulic permeabilities of the channel and the lipid bilayer. Also, as soon as the osmoticant is added, it enters the vesicle through channels, and water follows. Changes in volume are minimal.

After the vesicle does reswell to its initial volume, further water entry results in a rapid, effectively instantaneous, development of a ΔP. This is the result of the indistensibility of the vesicle membrane ($J_v = 0$). In experimental practice, the membrane can expand by ~3% before rupturing (Evans and Skalak, 1983), rather than being totally indistensible, as we have modeled it. The time course for the development of the intravesicular ΔP is then determined by the elasticity of the membrane and the rate of its deformation. ΔP will still develop as osmoticant continues to enter the vesicle, but its time course will be slowed somewhat as the membrane elastically expands. Nonetheless, ΔP development in this system is very rapid.

ΔP drives water out of the vesicle through the channel, sweeping osmoticant along with it. Note that the water-coupled solute efflux is significant even when the steady-state pressure is not a function of σ (e.g., for porin channels as we have modeled them and with the solutes we consider). For KCl, for instance, which is impermeant through the bilayer, this is the only efflux of solute that balances the diffusive influx.

The Dependence of Fusion Rate on the Osmoticant Permeability

The model enables us to explain the observation that an osmoticant's ability to cause fusion is related to its permeability through lipid bilayer and the type of channel in the vesicles. With porin, 200 mosmol of osmoticants with low permeabilities through lipid bilayer (e.g., urea) produce fusion, whereas more permeant osmoticants, such as formamide and ethylene glycol, are ineffective at concentrations up to 750 mosmol (Akabas et al., 1984). Fusion with these permeant osmoticants often requires gradients as high as 2.0–3.0 osmol (Cohen et al., 1989).

As seen in Fig. 9 *C*, at a fixed channel density, the ΔP's produced by urea and KCl are ten to twenty times the ΔP's produced by the same gradient of formamide or ethylene glycol. Even at optimum channel densities, these latter solutes are less effective than the former, because of the leakiness of the contact region to these solutes. In experimental practice, vesicles can be reconstituted with only a fixed (yet unknown) density of porin channels. This density is unlikely to be optimized for the most permeant osmoticants and may be at the low range, where differences between the osmoticants may be greater than a factor of ten. Thus, very large osmotic gradients of the permeant solutes are required to develop a ΔP sufficient for fusion.

Whether the low channel densities arise from a low efficiency of porin reconstitution into small vesicles or a large vesicle radius is unknown (but see below).

When nystatin, a less permeable channel was used, the leaky solutes such as formamide were relatively effective in promoting fusion (Cohen et al., 1989). This occurred because swelling was not limited by the density of nystatin channels in the vesicles. The vesicles were formed with internal nystatin; nystatin monomers were then added to the bathing solution. As nystatin monomers continually partitioned into the vesicle membrane and aggregated to form channels, the number of nystatin channels spanning the membrane was always increasing. Eventually, the density corresponding to the maximum ΔP of the osmoticant was reached. Even though the values of ΔP_{max} are different for urea and formamide, they are both sufficient to lyse the vesicles. Furthermore, the vesicles used in these experiments were large in radius, often exceeding 4 μm. Since these vesicles sustain lower pressures when they lyse (see below), the pressures achieved with each osmoticant were sufficient to cause fusion in experimental practice.

When an impermeant solute bathing the vesicles was replaced by an isosmotic quantity of a permeant solute, urea was only slightly more effective than formamide in promoting fusion with porin as the channel (Cohen et al., 1989). This is predicted by the model (case IV). In summary, quantitatively the pressures calculated from the model predict the rates of fusion, assuming that the pressure drives fusion.

Are the Pressures Large Enough to Burst the Vesicle?

Given that osmotic swelling does generate an intravesicular ΔP, is ΔP sufficient to lyse the vesicle? PC vesicles have been measured to lyse when their tensions (T) attain values of 3 dyn/cm (erg/cm^2) (Evans and Skalak, 1983). According to LaPlace's law, the pressure sustained across a spherical membrane with a tension T is given by $\Delta P = 2T/r$. For vesicles 0.05, 0.25, and 1 μm in radius, the intravesicular ΔPs at lysis are 1.2, 0.24, and 0.06 atm. The ΔP generated by a 200 mosmol osmotic gradient of 100 mM KCl, which is the minimum gradient necessary to obtain fusion (Akabas et al., 1984), is 0.95 atm for a 0.05-μm-radius vesicle containing one porin channel. This is insufficient to lyse the 0.05-μm vesicle if the lysis tension is 3, but it is sufficient if T is less than 2.5 dyn/cm. For a 1-μm vesicle with one porin channel in a 100-mM-KCl gradient, however, the resulting ΔP is more than adequate to lyse the vesicle. These findings lead us to conclude that fusion of larger vesicles was optimized in the fusion experiments conducted with the minimum osmotic gradient. In these experiments the vesicles were prepared by either sonication-freeze-thaw or detergent dialysis, which produce vesicles with radii ranging from 0.04 to 0.3 μm (Cohen et al., 1984). Moreover, the channel densities in the resulting vesicles were not quantitatively well controlled in these preparations.

Implications for Reconstitution by Fusion

In the model system, the density of channels in the vesicle membrane ultimately determines the steady-state ΔP. This imposes limits on both the number and permeability properties of channels required to develop a ΔP. For very large and porous channels, such as porin, the maximum ΔP is reached with few channels in the vesicle. More channels increase the permeability to water, which dissipates the ΔP.

Small channels allow control of the ΔP provided that a large number can be incorporated into the vesicles. An efficacious channel is nystatin, the monomeric components of which are water soluble and can be included with the internal contents of the vesicles. Nystatin can be added to the vesicle-containing compartment at sufficient quantity to ensure that tens of thousands channels form in each vesicle (if the osmoticant is the bilayer-impermeant KCl, only one channel is needed). A typical bath concentration of nystatin that does cause fusion of vesicles is 60 μg/ml (Niles and Cohen, 1987).

Biological Significance

That swelling of vesicles is involved in secretion has been noted for at least seventy years (Loeb, 1919). While much evidence has accumulated that is consistent with the idea that in cells swelling causes fusion (Finkelstein et al., 1986), recent experiments argue that in mast cells from beige mice the fusion event is not triggered by swelling or generation of an intravesicular pressure (Breckenridge and Almers, 1987; Zimmerberg et al., 1987). In these experiments, secretion was induced by GTP-γS that was introduced into the cell via a patch pipette. In this system, secretion which is not triggered by Ca^{2+}, occurs with a time course of seconds, and biochemical events can occur throughout the cytoplasm. In nerve, on the other hand, secretion is triggered rapidly by Ca^{2+} entering through channels that are perhaps situated at the vesicular docking sites (Pumplin et al., 1981), synaptic delays range from 0.4 to 4 ms at 20°C (Katz and Miledi, 1965) (conditions have been established wherein secretion may occur as quickly as 200 μs after stimulation [Llinas et al., 1981]), and actions are local. We consider two classes of models for water movement promoting fusion and note some quantitative consequences.

It has been pointed out that if a rise in intracellular Ca^{2+} increased the permeability of the vesicle membrane to ions (Cohen et al., 1980; Cohen et al., 1982), say by opening Ca^{2+}-activated K^+ or other channels (Akabas et al., 1984; Stanley and Ehrenstein, 1985), osmotic swelling could, in principle, drive fusion. This would correspond to case IV. Consider a fully swollen vesicle with a radius of 30 nm. It has a volume of 1.13×10^{-16} ml. For concreteness, let the vesicle contain 280 mosmol (c_i) of an impermeant solute ($\sigma = 1.0$), be bathed by 280 mosmol (c_o) of solute which permeates a vesicular channel that is opened by Ca^{2+}, and the solute (not necessarily an electrolyte) has a $\sigma = 0.1$ within the channel. If the channel has an $L_p = 10^{-21}$ cm^6/erg·s (comparable to a porin channel), then the initial volume flux into the vesicle is $J_v = L_pRT(c_i - \sigma c_o) = 6.22 \times 10^{-15}$ ml/s. The vesicle's membrane can expand by 3% before bursting (Evans and Skalak, 1983), that is, the volume can expand ~4.5% or 5.09×10^{-18} ml. Using the initial rate of volume flux for simplicity, the vesicle will lyse or fuse 818 μs after the channel opens. If two such channels are simultaneously opened, the vesicle will burst in 409 μs, a value well within the range of synaptic delays. Thus, the instantaneous opening of vesicular channels by Ca^{2+} (but not Ca^{2+}-activated K^+ channels, which have slow activation kinetics [Moczydlowski and Latorre, 1983] and are probably not involved in fusion) is, therefore, a physically plausible mechanism for driving fusion.

There can be an aqueous space between a vesicle and plasma membrane, which we term a "corridor." In the case of a vesicle fusing to a planar membrane, the

osmotic forces create an intravesicular hydrostatic pressure and do not promote removal of water from the corridor (Cohen et al., 1989). It has been argued that for fusion of a bulged black lipid membrane to a bulged black lipid membrane osmotic conditions need to be established to remove water from the corridor between the membranes (Fisher and Parker, 1984). It has been suggested that in cells, movement of water from the corridor into the vesicle promotes dehydration of this region, and thereby fusion (Ehrenstein and Stanley, 1988). It is easy to hypothesize the simple scenario that the localized influx of Ca^{2+} opens vesicular channels facing the corridor, allowing solute influx from the small corridor into the vesicle, with water following, thereby promoting dehydration of the corridor; this, however, is unlikely. Although the volume of the corridor is significantly less than that of the vesicle, even if solute moves only from the corridor into the vesicle, predominantly cytoplasmic water (in addition to insignificant corridor water) enters the vesicle and the corridor will not become further dehydrated. We do note, however, that if channels such as those considered above are opened by the local influx of Ca^{2+}, and if the vesicular contents are impermeant and a cytoplasmic solute is permeant, then, in this case, water from only the corridor enters the vesicle, because the Ca^{2+}-opened channels face the corridor. Again, $J_v = L_p RT(c_i - \sigma c_0) = 6.22 \times 10^{-15}$ ml/s. If the corridor has a thickness (d) of 1 nm and a width (w) of 10 nm, and a length (l) equal to w, its volume is on the order of 10^{-19} ml. The water from the corridor can be depleted within 15 μs, assuming this water is not replenished by cytosolic water. This assumption, however, is unlikely.

The hydrodynamic permeability of the corridor (L_p^{cor}) can be approximated by $wd^3/12l\eta = 10^{-20}$ cm^6/erg·s, where η is the viscosity of water (Akabas et al., 1984), whereas L_p of porin is 10^{-21} cm^6/erg·s. At steady state, the flow of water from the cytosol into the corridor equals the flow from the corridor into the vesicle. The steady-state pressure within the corridor (ΔP_c) is given by $\Delta P_v L_p/(L_p + L_p^{cor})$ where ΔP_v is the intravesicular pressure. If $\Delta P_v = 10^6$ dyn/cm^2, then $\Delta P_c = 10^5$ dyn/cm^2. The compressibility K is denoted by $-1/V\, dV/dP$, and, for water, $K_w = 4.6 \times 10^{-11}$ cm^2/dyn (Weast, 1976). It follows that a ΔP_c of 10^5 dyn/cm^2 would be established in the corridor if its volume of 10^{-19} ml were to be depleted (without replenishment) by only 5×10^{-25} ml. Because the volume flux into the corridor given by $L_p^{cor}\, \Delta P_c$ equals 10^{-15} ml/s at steady state, it takes ~0.5 ns for steady state to be established. This almost instantaneous replenishment of water in the corridor occurs because water is virtually incompressible. Therefore, osmotically dehydrating the corridor and thereby promoting fusion by this mechanism is improbable.

APPENDIX

Water and solute permeability data for nystatin channels are available (Holz and Finkelstein, 1970; Finkelstein and Holz, 1973; Kleinberg and Finkelstein, 1984) and are compiled in Finkelstein (1987). While permeability coefficients have not been determined for porin channels, a sieving diameter of 11.6 Å has been measured (Nikaido and Rosenberg, 1981). The permeability coefficients calculated below are for single channels. When more than one channel is present, the total permeability coefficient is that for the single channel multiplied by the number of channels.

Water Permeabilities

Nystatin. The single channel L_p is calculated from the relation $L_pRT = \bar{p} \cdot \bar{V}_w$ where $\bar{p}$ is the filtration permeability of the channel. $\bar{p} = 1.5 \times 10^{-14}$ cm^3/s for double-sided nystatin channels (Finkelstein, 1987).

Porin. L_p is estimated from Poisseuille's law, $L_p = \pi r^4/8l\eta$, where the length of the channel is taken as 5 nm, the radius of the channel is set at 5.8 Å, and the viscosity of water $\eta = 0.85$ cp. Justification for using Poisseuille's law is given in Finkelstein (1987). Values of L_p are given in Table AI.

Solute Permeabilities

We separately consider nonelectrolytes and salts as osmoticants.

Nonelectrolytes. ω_p's for urea and ethylene glycol through nystatin channels were obtained from $\omega_p = \bar{p}_d/RT$, where $\bar{p}_d$ is the solute permeability coefficient of a single double-sided nystatin channel. The $\bar{p}_d$ for urea is 3.6×10^{-16} cm^3/s (Kleinberg and Finkelstein, 1984). The $\bar{p}_d$ for ethylene glycol was obtained by scaling the $\bar{p}_d$ for urea by the factor 0.47, which is the ratio of their solute permeability coefficients, P_d(ethylene glycol)/P_d(urea), measured for nystatin-treated membranes (Holz and Finkelstein, 1970). The ω_p for formamide is estimated to be 2.11 (i.e., 1/0.47) times as large as that of urea, because it is smaller than urea by about the same factor that urea is smaller than ethylene glycol.

TABLE AI

Estimated Single-Channel Values of L_p for Porin and Nystatin

Channel	L_p (cm^6 · erg^{-1} · s^{-1})	
	Measured	Poisseuille
Nystatin*	1.08×10^{-25}	
Porin		1.05×10^{-21}

*Finkelstein, 1987.

The porin channel was modeled as a water-filled pipe through which solute permeates by diffusion. To bound the range of possible ω_p's, permeability coefficients were estimated in two ways. The larger estimates of ω_p treat solute movement as free diffusion. $\bar{p}_d = D \cdot A/l$, where D is the diffusion constant of the solute in water calculated by the Stokes-Einstein relation and A is the cross-sectional area of the channel ($A = \pi \cdot r^2$, where $r = 5.8$ Å). The lower estimates of ω_p account for solute interactions with the wall of the channel as calculated by Renkin (1954). The interaction amounts to steric hindrance of the solute as it traverses the water-filled lumen of the channel and so is based on macroscopic considerations. This method multiplies the free diffusion values by the factor R given by:

$$R = (1 - g)^2 \cdot (1 - 2.104g + 2.09g^3 - 0.95g^5), \tag{1A}$$

where $g = a_o/r$, in which a_o is the molecular radius of the solute as given by Renkin (1954). ω_p's are listed in Table AII.

Salts. Nystatin and porin are permeable to both anions and cations. The codirectional movement of anions and cations through the channels is coupled by the electric field established by the space-charge region that results from the ions' differing mobilities. We calculated the permeability of the salt ($\bar{p}$) by a modified Nernst-Planck equation, $\bar{p} = 2t_+t_- RT/F^2c \cdot g$, where t_+ and t_- are dimensionless transference numbers for the cation and anion within the channel, respectively (Finkelstein and Mauro, 1977), g is the single-channel con-

TABLE AII

Estimated Single-Channel Values of ω_p for Nystatin and Porin

Method	Osmoticant	ω_p (per channel)	
		Nystatin	Porin
Free diffusion	Urea		1.18×10^{-23}
	Formamide		1.45×10^{-23}
	Ethylene glycol		1.07×10^{-23}
Corrected diffusion	Urea		8.05×10^{-25}
	Formamide		1.14×10^{-24}
	Ethylene glycol		5.47×10^{-25}
Measured*	Urea	1.44×10^{-26}	
	Formamide	3.03×10^{-26}	
	Ethylene glycol	6.82×10^{-27}	
Nernst-Planck	KCl	1.40×10^{-27}	5.52×10^{-24}

The units of ω_p are mol · cm^3/erg · s or mol · cm · s/g.

*The value for urea is taken from Kleinberg and Finkelstein, 1984. The single-channel permeability to ethylene glycol was calculated from the urea-to-ethylene glycol ratio of macroscopic permeability coefficients measured for a nystatin-treated membrane (Holz and Finkelstein, 1970). The permeability to formamide was estimated on the basis of this ratio and the molecular radii of formamide and urea.

ductance, F is Faraday's constant, and c is the concentration of permeating salt. t_+/t_- (the cation-to-anion selectivity) was determined from the measured reversal potentials for nystatin (Kleinberg and Finkelstein, 1984) and *Escherichia coli* porin (Benz et al., 1979) using the Goldman-Hodgkin-Katz equation. Values for KCl obtained by this ad hoc method are given in Table AII.

Reflection coefficients. For nystatin channels, measured values were used for the reflection coefficients of the osmoticants (Holz and Finkelstein, 1970) unless otherwise indicated. σ was usually fixed arbitrarily at 0.1 for all solutes through the porin channel.

This study was supported by National Institutes of Health grants GM-27367, GM-29210, and 5F32 GM-08549.

Original version received 19 April 1988 and accepted version received 25 July 1988.

REFERENCES

Akabas, M. H., F. S. Cohen, and A. Finkelstein. 1984. Separation of the osmotically driven fusion event from vesicle-planar membrane attachment in a model system of exocytosis. *Journal of Cell Biology.* 98:1063–1071.

Benz, R., K. Janko, and P. Läuger. 1979. Ionic selectivity of pores formed by the matrix protein (porin) of *Escherichia coli*. *Biochimica et Biophysica Acta.* 551:238–247.

Breckenridge, L. J., and W. Almers. 1987. Final steps in exocytosis observed in a cell with giant secretory granules. *Proceedings of the National Academy of Sciences.* 84:1945–1949.

Cass, A., and A. Finkelstein. 1967. Water permeability of thin lipid membranes. *Journal of General Physiology.* 50:1765–1784.

Cohen, F. S. 1986. Fusion of liposomes to planar bilayers. *In* Ion Channel Reconstitution. C. Miller, editor. Plenum Publishing Corp., New York. 131–139.

Cohen, F. S., M. H. Akabas, and A. Finkelstein. 1982. Osmotic swelling of phospholipid vesicles causes them to fuse with a planar phospholipid bilayer membrane. *Science.* 217:458–460.

Cohen, F. S., M. H. Akabas, J. Zimmerberg, and A. Finkelstein 1984. Parameters affecting the fusion of unilamellar phospholipid vesicles with planar bilayer membranes. *Journal of Cell Biology.* 98:1054–1062.

Cohen, F. S., W. D. Niles, and M. H. Akabas. 1989. The magnitude of the osmotic gradient required for the fusion of phospholipid vesicles with a planar phospholipid bilayer depends on the membrane permeability of the solute used to creat the osmotic pressure. *Journal of General Physiology.* 93:000–000.

Cohen, F. S., J. Zimmerberg, and A. Finkelstein. 1980. Fusion of phospholipid vesicles with planar bilayer membranes. II. Incorporation of a vesicular membrane marker into the planar membrane. *Journal of General Physiology.* 75:251–270.

Ehrenstein, G., and E. F. Stanley. 1988. Hypothesis: An increase in osmolarity of secretory vesicles triggers exocytosis by reducing the distance between the vesicles and the plasma membrane. *Biophysical Journal.* 53:10*a*. (Abstr.)

Evans, E. A., and R. Skalak. 1983. Mechanics and Thermodynamics of Biomembranes. CRC Press, Inc., Boca Raton. 148.

Fettiplace, R., and D. A. Haydon. 1980. Water permeability of lipid membranes. *Physiological Reviews.* 60:510–550.

Finkelstein, A. 1976. Water and nonelectrolyte permeability of lipid bilayer membranes. *Journal of General Physiology.* 68:127–135.

Finkelstein, A. 1987. Water movement through lipid bilayers, pores and plasma membranes. Theory and reality. *In* Distinguished Lecture Series of the Society of General Physiologists. John Wiley & Sons, Inc., New York. 228 pp.

Finkelstein, A., and R. Holz. 1973. Aqueous pores created in thin lipid membranes by the polyene antibiotics nystatin and amphotericin B. *In* Membranes, A Series of Advances. Vol. 2. Lipid Bilayers and Antibiotics. G. Eisenman, editor. Marcel Dekker, Inc., New York. 377–408.

Finkelstein, A., and A. Mauro. 1981. Physical principles and formalisms of electrical excitability. *In* Handbook of Physiology. The Nervous System I. American Physiological Society, Washington, D.C. 161–213.

Finkelstein, A., J. Zimmerberg, and F. S. Cohen. 1986. Osmotic swelling of vesicles: its role in the fusion of vesicles with planar phospholipid bilayer membranes and its possible role in exocytosis. *Annual Review of Physiology.* 48:163–174.

Fisher, L. R., and N. S. Parker. 1984. Osmotic control of bilayer fusion. *Biophysical Journal.* 46:253–258.

Hartshorne, R. P., B. U. Keller, J. A. Talvenheimo, W. A. Catterall, and M. Montal. 1985. Functional reconstruction of the purified brain sodium channel in planar lipid bilayers. *Proceedings of the National Academy of Sciences.* 82:240–244.

Holz, R., and A. Finkelstein. 1970. The water and nonelectrolyte permeability induced in thin lipid membranes by the polyene antibiotics nystatin and amphotericin B. *Journal of General Physiology.* 56:125–145.

Katz, B., and R. Miledi. 1965. The measurement of the synaptic delay, and the time course of acetylcholine release at the neuromuscular junction. *Proceedings of the Royal Society (London) Series B.* 161:483–495.

Kedem O., and A. Katchalsky. 1958. Thermodynamic analysis of the permeability of biological membranes to non-electrolytes. *Biochimica et Biophysica Acta.* 27:229–246.

Kleinberg, M. E., and A. Finkelstein. 1984. Single-length and double-length channels formed by nystatin in lipid bilayer membranes. *Journal of Membrane Biology.* 80:257–269.

Llinas, R., I. Z. Steinberg, and K. Walton. 1981. Relationship between presynaptic calcium current and postsynaptic potential in squid giant synapse. *Biophysical Journal.* 33:323–352.

Loeb, J. 1919. Artificial Parthenogenesis and Fertilization. Chicago University Press, Chicago. 209–210.

Moczydlowski, E., and R. Latorre. 1983. Gating kinetics of Ca^{2+}-activated K^+ channels from rat muscle incorporated into planar bilayers: evidence for two voltage-dependent Ca^{2+} binding reactions. *Journal of General Physiology.* 82:511–542.

Nikaido, H., and E. Y. Rosenberg. 1981. Effect of solute size on diffusion rates through the transmembrane pores of the outer membrane of *Escherichia coli. Journal of General Physiology.* 77:121–135.

Niles, W. D., and F. S. Cohen. 1987. Video fluorescence microscopy studies of phospholipid vesicle fusion with a planar phospholipid membrane. Nature of membrane-membrane interactions and detection of release of contents. *Journal of General Physiology.* 90:703–735.

Orbach, E., and A. Finkelstein. 1980. The nonelectrolyte permeability of planar lipid bilayer membranes. *Journal of General Physiology.* 75:427–436.

Pumplin, D. W., T. S. Reese, and R. Llinas. 1981. Are the presynaptic membrane particles the calcium channels? *Proceedings of the National Academy of Sciences.* 78:7210–7213.

Renkin, E. M. 1954. Filtration, diffusion, and molecular sieving through porous cellulose membranes. *Journal of General Physiology.* 38:225–243.

Stanley, E. F., and G. Ehrenstein. 1985. A model for exocytosis based on the opening of calcium-activated potassium channels in vesicles. *Life Sciences.* 37:1985–1995.

Walter, A., and J. Gutknecht. 1986. Permeability of small nonelectrolytes through lipid bilayer membranes. *Journal of Membrane Biology.* 90:207–217.

Weast, R. C., editor. 1976. *Handbook of Chemistry and Physics.* CRC Press, Inc., Cleveland. F–21.

Woodbury, D. J. 1986. Fusion of vesicles with planar bilayers: membrane fusion and content release. Ph.D. dissertion. University of California, Irvine, CA.

Zimmerberg, J., F. S. Cohen, and A. Finkelstein. 1980. Fusion of phospholipid vesicles with planar phospholipid bilayer membranes. I. Discharge of vesicular contents across the planar membrane. *Journal of General Physiology.* 75:241–250.

Zimmerberg, J., M. Curran, F. S. Cohen, and M. Brodwick. 1987. Simultaneous electrical and optical measurements show that membrane fusion precedes secretory granule swelling during exocytosis of beige mouse mast cells. *Proceedings of the National Academy of Science.* 84:1585–1589.